



Integrated Arctic Observation System

Research and Innovation Action under EC Horizon2020

Grant Agreement no. 727890

Project coordinator:

Nansen Environmental and Remote Sensing Center, Norway

Deliverable 6.16

Natural Hazard Assessment in the Arctic

Start date of project:	01 December 2016	Duration:	60 months
Due date of deliverable:	30 September 2021	Actual submission date:	30 June 2021
Lead beneficiary for preparing the deliverable:	GEUS		
Person-months used to produce deliverable:	31 pm		

Authors: Anne Solgaard, Andreas Ahlstrøm, Kenneth Mankoff, Francisco Navarro, Eva De Andrés, María Isabel de Corcuera, Jaime Otero, Roberta Pirazzini, Ilona Valisuo, Holt Hancock, Laura Rontu, Elena Shevnina, Shfaqat Abbas Khan, Mathilde B. Sørensen, Peter H. Voss
Reviewer: Geir Ottersen

Version			
1.0	DATE	CHANGE RECORDS	LEAD AUTHOR
1.1	01.04.2020	Template	A. Solgaard
1.2	07.06.2021	1st Draft	All
1.3	15.06.2021	Revision by partners	All
1.4	23.06.2021	Internal revision	G. Ottersen, A. Solgaard
1.5	30.06.2021	Technical revision and submission	K. Lygre

Approval X	Date:	Sign.
	1 July 2021	 Stein Sandven (Coordinator)

USED PERSON-MONTHS FOR WRITING THIS DELIVERABLE					
No	Beneficiary	PM	No	Beneficiary	PM
1	NERSC		24	TDUE	
2	UiB	1	25	GINR	
3	IMR		48	UNEXE	
4	MISU		27	NIVA	
5	AWI		28	CNRS	
6	IOPAN		29	U Helsinki	
7	DTU	5	30	GFZ	
8	AU		31	ARMINES	
9	GEUS	14	32	IGPAN	
10	FMI	7	33	U SLASKI	
11	UNIS	0.2	34	BSC	
12	NORDECO		35	DNV GL	
13	SMHI		36	RIHMI-WDC	
14	USFD		37	NIERSC	
15	NUIM		38	WHOI	
16	IFREMER		39	SIO	
17	MPG		40	UAF	
18	EUROGOOS		41	U Laval	
19	EUROCEAN		42	ONC	
20	UPM	4	43	NMEFC	
21	UB		44	RADI	
22	UHAM		45	KOPRI	
23	NORCE		46	NIPR	
			47	PRIC	

Person months include also all underlying work leading up to the work with the deliverable

DISSEMINATION LEVEL		
PU	Public, fully open	X
CO	Confidential, restricted under conditions set out in Model Grant Agreement	
CI	Classified, information as referred to in Commission Decision 2001/844/EC	

EXECUTIVE SUMMARY

This document, **Deliverable 6.16 - Natural Hazard Assessment in the Arctic**, describes the main body of work carried out in task 6.4 Natural hazards in the Arctic.

This document is intended to:

- Describe the needs of the stakeholders.
- Provide a description of the individual studies in the task and how data and methods from the iAOS advances our understanding of the selected hazards.
- Discuss which stakeholder needs are met and what is still required in cases where they are not.
- Provide input to the INTAROS roadmap based on the work on natural hazards in the Arctic.

1. Table of Contents

1. Table of Contents	3
2. Introduction: Natural Hazards in the Arctic	5
3. Stakeholder Needs	6
3.1. Snow avalanche	6
3.2. Earthquake, Landslide, tsunami	7
3.3. Mass loss from ice sheets and glaciers	7
4. Description of work	9
4.1. Snow avalanche	9
4.2. Earthquake, landslide, tsunami	13
4.3. Mass loss from ice sheets and glaciers	16
4.3.1. Sea level: Mass change	17
4.3.2. Sea level: Input/output	19
4.3.3. Solid ice discharge	20

4.3.4. Error estimates for solid ice discharge to the ocean	21
4.3.5. Partitioning of ice discharge into iceberg calving and submarine melting	24
4.3.6. Freshwater runoff	26
5. Synthesis on achievements concerning stakeholder needs and data gaps	27
5.1. Snow avalanche	27
5.2. Earthquake, landslide, tsunami	28
5.3. Mass loss from ice sheets and glaciers	29
6. Recommendations to Roadmap	31
6.1. Long time series	32
6.2. Services in real time	32
6.3. Availability of datasets	33
6.4. Super sites with multi-disciplinary observations	33
6.5. Citizen Science	35
7. Summary	36
8. Literature	38

2. Introduction: Natural Hazards in the Arctic

The INTAROS project provides a wealth of data and tools available through the integrated Arctic Observing System (iAOS). The aim of INTAROS Task 6.4 “Natural Hazards in the Arctic” is to demonstrate how the iAOS can be exploited to better understand natural hazards in the Arctic. In order to best showcase the value of the iAOS for this purpose, the work focuses on selected types of hazards, namely:

- Snow avalanches
- Earthquakes, landslides, and tsunamis
- Mass loss from ice sheets and glaciers: Sea level rise and freshwater discharge

Some natural hazards in the Arctic have their origin in the region, but mainly represent a hazard to people outside the region, such as the mass loss from ice sheets and glaciers causing regionally differentiated sea level rise across the world due to the changes caused in the gravitational fingerprint. This implies, for example, that low-lying countries like Bangladesh, Vietnam or the Maldives are experiencing a faster sea level rise due to Arctic land ice mass loss than the global average, while coastal Greenland is posed to experience a relative sea level lowering.

Other natural hazards in the Arctic are due to local phenomena, like the avalanche risk in Longyearbyen, which may be exasperated by the accelerated climate change experienced in the Arctic, or seismically active regions where more accurate mapping of seismic events can point out areas prone to earthquakes and landslides or derived risks like tsunamis. Changes in the freshwater flux into fjords stemming from icebergs and surface meltwater from glaciers further constitutes a hazard to the local marine ecosystem.

The selection of natural hazards addressed here, demonstrates the potential of the synergetic approach of the project in providing innovative services across a broad range of applications.

This report contains a description of the activities carried out in task 6.4. The aim of the document is to report the work performed in the task and to provide the context of each selected hazard with focus on the identified stakeholder needs, how these are or can be fulfilled as well as to provide input to the INTAROS roadmap. The document is structured as follows:

Chapter 2 contains an introduction to the document.

Chapter 3 describes the stakeholder needs.

Chapter 4 contains a description of the work carried out within Task 6.4 for each hazard.

Chapter 5 discusses how well the stakeholder needs is fulfilled by the work performed in Task 6.4

Chapter 6 contains the recommendations to the INTAROS roadmap based on the results and knowledge gained from the work in Task 6.4.

3. Stakeholder Needs

This section describes the data sets, knowledge gaps and/or difficulties that are missing for stakeholders like local communities, policy makers or scientists to move forward.

3.1. Snow avalanche

Extreme cyclone events (sometimes called 'weather bombs') over Svalbard are increasing by about 3-4 events per decade in November-December (Rinke et al., 2017) in association to the decreasing sea ice extent and the change in atmospheric circulation pattern. Heavy precipitation, in the form of snow or rain, generally occurs during these extreme events, challenging infrastructures and local communities because of the high risks of avalanches and landslides.

Avalanche forecast models require input from numerical weather prediction models, which, however, cannot resolve the complex Svalbard topography and therefore cannot provide accurate snow precipitation and snow accumulation in the mountain slopes where avalanches can take place. In Svalbard snow distribution patterns are controlled by winds, and snowfall accompanied by strong winds from a specific direction can be a precursor for avalanches (Hancock et al. 2018). Based on these findings, our objective here is to derive statistical relationships between in-situ measurements and model data of snow and weather conditions to improve the snow accumulation forecast. These relationships can then be applied in snow models to improve the avalanche risk assessment. This method would require a long time series of collocated snow and meteorological observations which, however, are not available. After the disastrous snow avalanche at the end of 2015, automatic snow depth stations have been deployed by UNIS in the snow release areas around Longyearbyen, and these data are transferred to the Skred AS consulting company, a subcontractor of the Norwegian Water Resources and Energy Directorate (NVE) responsible for avalanche forecasts in Norway. However, the stations are still at an experimental phase, their location and instruments are often changed after one or two years, and several of them have discontinuity in data recording. Moreover, the stations do not record wind speed and direction, which are key variables for snow accumulation modelling as they shape the local snow distribution. For this study, we selected the snow season 2017-2018 in which at least three snow stations with good quality data were available. After the data analysis, we provide recommendations on the dataset that would be needed to develop a more robust methodology.

3.2. Earthquake, Landslide, tsunami

To meet the stakeholder need of quantifying the risk of natural hazards, observation of previous hazardous events is mandatory. Observation of natural hazard events requires long-term continuous time series. Seismometers can provide information on earthquakes, but also on landslides, snow avalanches and, to some extent, tsunamis. The detection capacity of a seismic network is controlled by inter-station distance, the noise level at station locations and the quality of the equipment. Good detection requires a dense network of stations, also covering the ocean areas, at locations with a low noise level. Some stakeholders (e.g. communities) need clear information that can be implemented in decision making. This includes information on previous events, the potential for future events with associated uncertainties, as well as on the potential impact of events on societies and the environment. There is also a need for access to resources that are capable of processing and analyzing the collected data and evaluating the hazard. To meet the stakeholder need to be able to react quickly and adequately to hazardous events, real time data collection and transfer is required.

3.3. Mass loss from ice sheets and glaciers

Mass loss from glaciers and ice sheets from either melt or calving eventually ends up as a freshwater input to the oceans. It therefore constitutes both possible local and global hazards making it important to both local and global stakeholders.

The rise in the global mean sea level represents a natural hazard to coastal communities worldwide. As stated in the recent IPCC Special Report on the Ocean and Cryosphere in a Changing Climate: “Global mean sea level (GMSL) is rising (*virtually certain*) and accelerating (*high confidence*). The sum of glacier and ice sheet contributions is now the dominant source of GMSL rise (*very high confidence*).” (Meredith et al., 2019: IPCC Chap. 3). Implications are far reaching and adaptation measures are increasingly difficult as also stated in the Arctic Monitoring and Assessment Report on ‘Snow, Water, Ice and Permafrost in the Arctic’ from 2017: “Coastal communities, low-lying islands, and ecosystems throughout the world will be affected by the melting of land ice (glaciers and ice sheets) in the Arctic, which is projected to increase the rate of global sea-level rise. Impacts include coastal flooding, erosion, damage to buildings and infrastructure, changes in ecosystems, and contamination of drinking water sources.” (AMAP, 2017). Increased global sea level due to melting glaciers and ice caps will in the future have a significant effect on sea level, with an irregular geographic distribution associated with change in the gravitational field by e.g. the Greenland ice mass loss.

The Greenland Ice Sheet currently contributes more to the ocean mass gain than any other source and is second in relevance - following thermal expansion of the oceans - concerning sea-level rise contribution (24% of total current sea-level rise, IPCC, 2019). Monitoring and understanding this mass loss from the ice sheet is essential in order to project its future contribution, yet even separating the mass loss between the main processes of surface mass balance (snowfall and melt) and marine mass loss (iceberg calving and glacier front melting in the ocean) remains elusive. Continued observations of ice-sheet-wide mass change and an improved understanding of the processes leading to this change are needed to improve projections.

Quantification of the mass loss from these processes on a high spatial and temporal scale is key to improve the performance of numerical models and is identified as a key gap. Addressing this gap will also facilitate improved modelling of other processes depending on the freshwater cycle in the coastal zone of Greenland, such as marine ecosystem modelling and ocean circulation modelling.

Process understanding, in turn, requires detailed models at the local scale, which must be fed by a variety of data which are seldom available. For instance, for analyzing the processes involved in the glacier-ocean interaction, which are crucial to understand the partitioning of mass losses from marine-terminating glaciers into iceberg calving and frontal submarine melting, plenty of data from both glacier, ocean and atmosphere are needed. These include, among others: 1) air temperature (preferably at various levels), precipitation (solid/liquid), wind velocity and direction (for snow redistribution) and radiation at the glacier surface; 2) accumulation and ablation measurements at various locations at the glacier surface; 3) glacier surface velocities from GNSS measurements; 4) detailed surface topography and ice-thickness data; 5) detailed fjord bathymetry; 6) CTD data at various locations at the fjord; 7) fjord water velocity at various depth levels, at least at the fjord mouth; 8) glacier front position changes; and 9) fjord ice mélange coverage. While some of these data can be obtained from remote sensing observations (e.g. satellite-derived ice surface velocities, front position changes) and from modelling (e.g. regional climate modelling), field data are still needed for coupled glacier-fjord model parameter calibration and validation of model results. Having available such an amount and variety of data is, of course, not feasible at a wide scale. But, thinking of process understanding, it is crucial to collect such data for a set of benchmark glacier/fjord systems or “supersites”. Here, the term “supersite” is defined as in INTAROS D2.10. Identifying such benchmark glaciers and completing the data lacking for them is an important gap that needs to be filled. The oceanographic data (CTD, currents) poses special challenges, given the ice-mélange coverage of most fjords.

Also, on the local scale, changes in the amount and timing of the freshwater input to fjords and near coastal waters impact the marine ecosystem and thus fishery which in turn may impact local economies. In addition, rapid land uplift in Greenland due to ice low may cause local deformation resulting in large earthquakes and tsunamis. Maps of uplift are needed to identify areas of risk.

Policymakers and coastal planners require an estimate as accurate as possible of the projected sea-level rise under various emission scenarios. Local communities rely on results from ecosystem models to plan for changes in fish stocks and on hazard maps for safety and securing infrastructure. These all require good quality, easily accessible and continuous monitoring of ice mass loss as well as a better process understanding. This also includes that data are provided at high temporal and spatial resolution. As the uncertainties are expected to be large, error estimates play a relevant role.

4. Description of work

This section describes the actual work carried out in INTAROS Task 6.4 using data or methods available from the iAOS.

4.1. Snow avalanche

We aim to derive statistical relationships between the in-situ measurements of snow depth and the meteorological parameters that affect the distribution of snow accumulation in the mountain slopes surrounding Longyearbyen. The calculations are done for the period from November 2017 to May 2018. We use automatic snow depth observations from three measurement stations (Lia, Nybyen and Sverdruphamaren) and meteorological data from two weather stations (Gruvefjellet Automatic Weather Station and Svalbard Airport Synop Station, Table 1). A map with the location of the station is given in Figure 1. We extract atmospheric model data from the Copernicus Arctic Regional Reanalysis (CARRA) at the grid points closest to the observation stations. CARRA uses the HARMONIE-AROME weather prediction system (Bengtsson et al., 2017) with boundary forcing from ERA5 reanalysis, 2.5km horizontal resolution, 3-dimensional variational assimilation, and 3-hourly update frequency for the assimilation.

Tabel 1: Name and position of the snow and weather stations that provided the utilized in-situ observations.

Station	Lon	Lat	Elevation (m asl)	Slope (steepness; facing)	Source
Lia (snow station)	15.648	8.215	121	34°; 315°	UNIS, Holt Hancock
Nybyen (snow station)	15.609	78.20	352	33°; 300°	UNIS, Holt Hancock
Sverdruphamaren (snow station)	15.567	78.21	450	39°; 110°	UNIS, Holt Hancock
Gruvefjellet (AWS)	15.617	78.20	464	flat	UNIS, https://www.unis.no/resources/weather-stations , Access date 9.2.2021
Svalbard Airport (AWS)	15.50	78.24	28	flat	Met No, http://eklima.met.no , Access date 4.2.2021

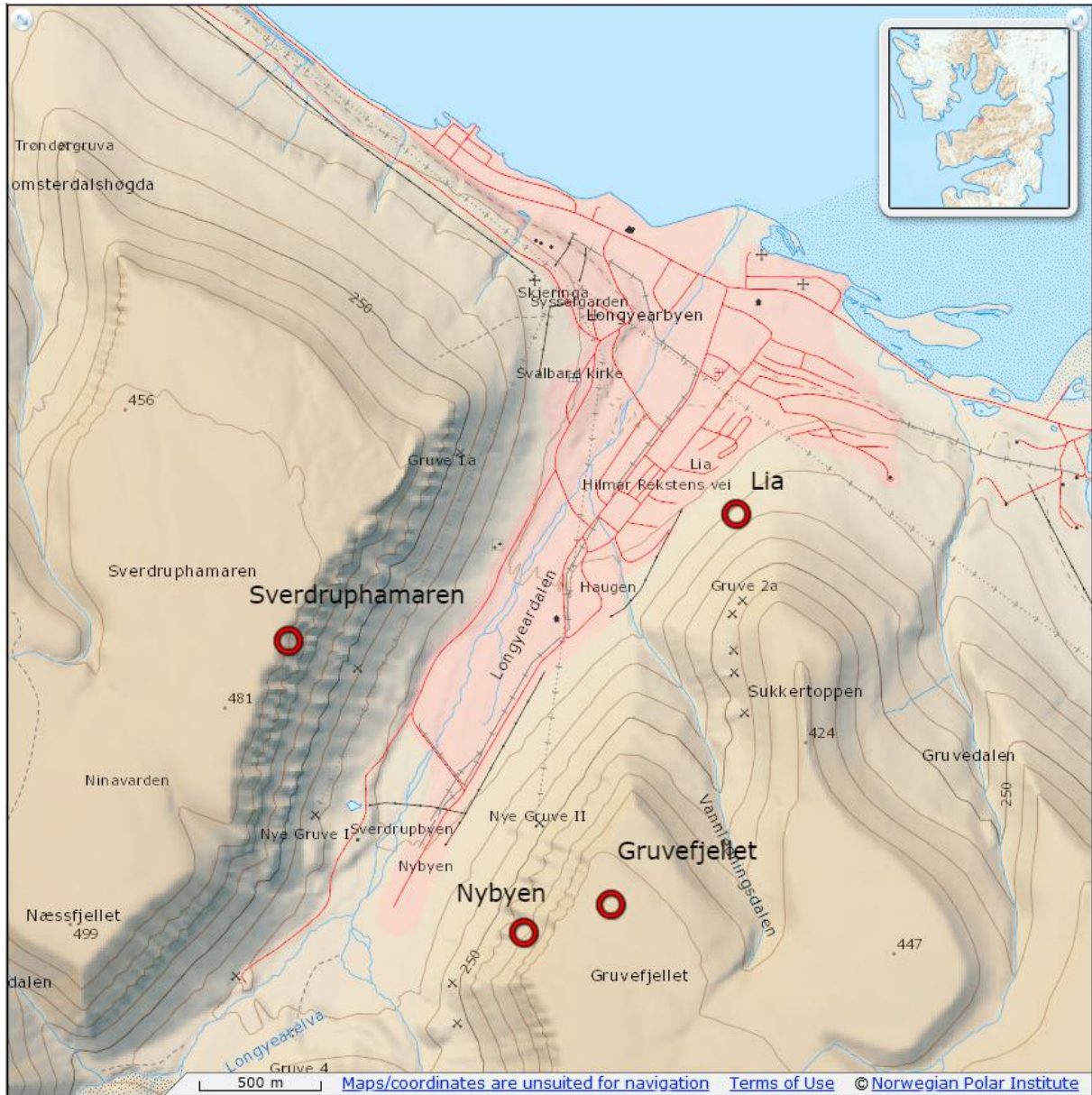


Figure 1: Map of the Longyeardalen valley with the location of the Longyearbyen town and of the utilized snow stations (Lia, Nybyen, and Sverdruphamaren) and of the closest automatic weather station (AWS) Gruvefjellet.

The match between observed weather conditions and CARRA is mostly good. The model tends to overestimate the 2 m temperature in cases of surface inversion and shows a systematic bias (model minus observations) in wind direction which is 17.6 degrees at Svalbard Airport and 36.9 degrees at Gruvefjellet (note that Svalbard Airport is assimilated in the model). Wind speed values match each other well with biases of 0.6 m/s at Svalbard Airport and 1.5 m/s at Gruvefjellet. The timing of precipitation events is coherent based on observations at Svalbard Airport. Snow conditions are more complex and modelled snow (amount of precipitation or modelled snow thickness) poorly matches with the observed snow thickness at the snow station locations. The snow thickness biases are in the order of tens of centimetres, easily reaching -50 cm (amount of snow accumulation underestimated in the model). This is expected as the stations are not representative for the model grid and demonstrates the need to correct the model snow in complex terrain. The lack of wind measurements at the snow sites prevents detailed studies on the effect of wind on snow accumulation at Lia and Sverdruphamaren. At Nybyen we can assess the relationship between snow depth evolution and wind conditions (Figure 2) using the Gruvefjellet weather station located 380m away. Precipitation (CARRA data) occurs mostly when winds are from two distinct directional sectors, 80-125 degrees (in the direction of the slope) and 175-250 degrees (along the Longyeardalen valley). Winds in the direction of the slope are associated with only minor changes in snow depth (both accumulation and erosion by drifting snow occur with equal frequency) and 2 m air temperature mostly below -5 °C. Winds along the Longyeardalen valley are associated with the strongest snow precipitation and accumulation events, with 2 m air temperature mostly above -5 °C. Only in case of strong wind speed (> 12 m/s) erosion prevailed over accumulation. Although the data covers only one season and the number of precipitation events is small (making it hard to determine robust statistical relationships between snow and weather conditions) these analyses identified the local atmospheric conditions in which snow erosion and accumulation are most probable on the slopes where snow avalanches have been observed in the past. This statistical tool should be refined with additional observations from longer time series and collocated meteorological and snow depth data.

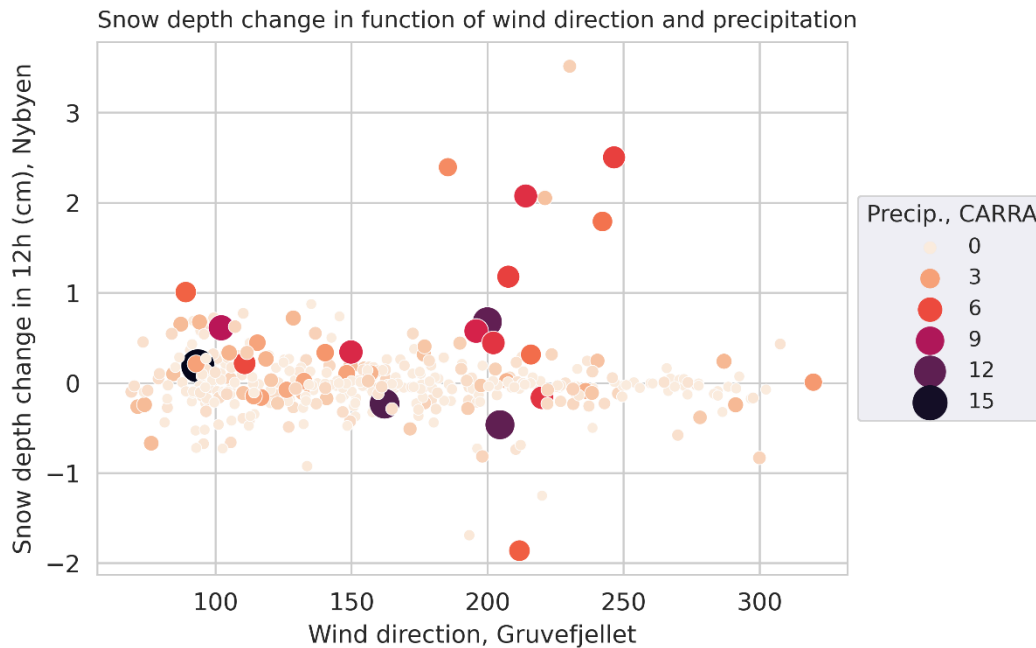


Figure 2: Modelled snow precipitation (mm/12h) on the closest model grid cell as a function of wind direction measured at Gruvefjellen station (x-axis) and snow depth change in 12 hours measured at Nybyen station (y-axis).

We also tested an empirical correction of the model precipitation using the observed snow depth evolution. Bellaire et al. (2011, corrigendum 2013) proposes three correction methods based on ratio (R) and difference (D) of modelled and observed precipitation, as well as one method based on constant (C) correction factor. These correction methods were modified to fit our data and tested on the three snow stations. The ratio method allowed to improve the correlation and to decrease the bias of model precipitation at all three stations. However, the results might be too optimistic, as now the correction function was tested on the same data that was used for deriving the corrections parameters. Nevertheless, it seems that there is potential for developing the methods further by adding weather-based correction factors to the method, for example a temperature based correction for temperatures above melting point, which are currently not represented in the correction method.

Snow avalanche forecasting in the Longyearbyen area is necessary to protect the population and the infrastructures concentrated at the bottom of the valley. The improvement of inputs to avalanche forecast models, as well as the testing and development of the snow model themselves, heavily rely on the availability of local observations of snow and meteorological variables, possibly existing as a long time series. Although this study could be based on a very limited dataset, it showed the potential of applying in situ observations to downscale or train the meteorological variables used as input to the snow model, highlighting the necessity of permanent snow and meteorological stations that could provide the time series needed for the development of the method.

To reinforce the above described statistical approach, we also utilized the geostatistical tool RIntaros/RGeostats developed by ParisTech and available in the iAOS, to produce gridded maps of snow depth on the Longyearbyen valley at high horizontal resolution (25 m). These maps can be extremely useful to validate the snow model applied for the avalanche forecast. To generate the dataset of snow depth maps, we utilized Arctic-AROME model output (2-m temperature, 10m-wind, precipitation, and other relevant model-derived information) which is analogous to the CARRA reanalysis products, as well as in situ 2-m temperature and wind speed from all available Automatic Weather Stations in the valley and in the adjacent areas and snow depth from the same three snow depth stations (Lia, Sverdruphamaren and Nybyen) utilized in the analysis described above. A detailed description of the snow map product and of the method to derive it is provided in deliverable D5.10.

4.2. Earthquake, landslide, tsunami

Monitoring of natural hazards (mostly earthquakes) is mainly based on seismic stations, though satellite systems are increasingly used as well (D2.9). Permanent seismic stations are currently restricted to land areas, leading to large monitoring gaps in the ocean areas. Even in the Arctic land areas, instrumentation is sparse due to logistical challenges.

In order to provide a baseline of seismological monitoring in the Arctic, catalogs of seismic events and seismological monitoring stations have been developed (D2.9) and published through the INTAROS catalog.

Various approaches have then been tested to improve the seismological monitoring of natural hazards in the Arctic. Community based seismometers have been demonstrated as a useful low-cost supplement to permanent seismic stations on land (Jeddi et al., 2020).

The monitoring gap in the ocean has been partially filled with ocean bottom seismometers (OBS) (D2.7). Such deployments are usually restricted to one-year duration, whereas long-term monitoring is needed for hazard and risk assessment. There is no real time data transfer for such systems, though this is a requirement for disaster management. In INTAROS, two OBS deployments on the mid-Atlantic ridge have improved our understanding of the ridge seismicity (Jeddi et al., 2021) and demonstrated how even very few stations can significantly improve earthquake detection and locations. Deployment and (especially) recovery of OBS systems is very challenging in ice-covered areas where two-ship operation with icebreakers and ROV is needed with current technology to prevent the instruments from being trapped under the ice. Real time data transfer would require significant technology development in terms of underwater communication, or deployment of cabled systems.

A large number of seismic events in Western Greenland have been studied, these events were caused by or were suspected to be linked to landslides in the areas. Some of these events were detected on the seismic network in the region, satellite data was then used to search for landslides that could be linked to the seismic events. Other events were observed in satellite data, the seismic data was then examined to see if seismic energy was released during the event. The work is presented in Svennevig et al. (2019, 2020a and 2020b).

Community based seismometers have contributed to better earthquake locations and raised awareness among community members, especially in Western Greenland. OBS deployments on the mid-Atlantic ridge have contributed to improved event detection and location, and thus to improved understanding of the seismic activity in the region. Such improved understanding is the first step towards improved hazard and risk analyses which are needed to guide any risk mitigation effort. Data from the OBS deployments will be made available through the UIB-NORSAR EIDA node web interface (<https://eida.geo.uib.no/webdc3/>).

The combination of seismic and satellite data provides accurate locations in time and space of landslide events, since the seismic data have high time resolution but low spatial resolution whereas the satellite data have a low time resolution but a high spatial resolution. The much more precise monitoring of landslides using seismic and satellite data combined, is providing new information on landslide prone areas and the frequency of landslides. This information is important in the evaluation of future landslide risk. Considering the tsunamigenic potential of some large landslides, it is important to understand the landslide risk even in remote and unpopulated areas.

The number and magnitudes of earthquakes within a region can be used to estimate the seismic hazard constituted by possible future earthquakes. From the iAOS one can extract the information on, among other, earthquake locations and magnitudes in the arctic region. It is also possible to get a quick overview of available monitoring stations, and thus available data for further analysis.

Via the INTAROS website one can access the web service to search and extract data from the earthquake catalogue. The web service is described in detail in the video found here:

<http://intaros.eu/news/recent-news/guided-tour-of-intaros-data-catalogue/>

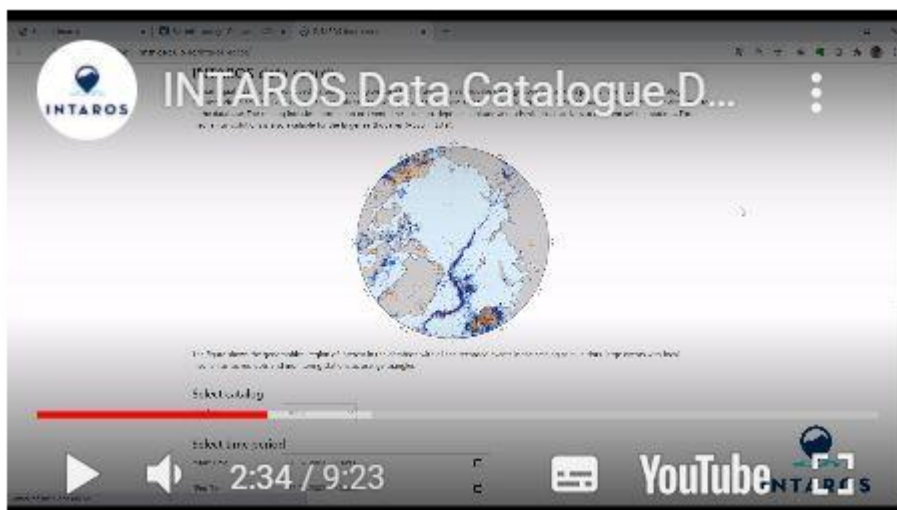


Figure 3: Video presentation on how to extract earthquake data from the iAOS.

In the following demonstration, we have extracted earthquakes in the period from primo JAN 2016 to ultimo FEB 2020, in a region around the Disco Bay, Greenland given by 66.5N to 72 N and 52 W to 50 W, see Figure 4.

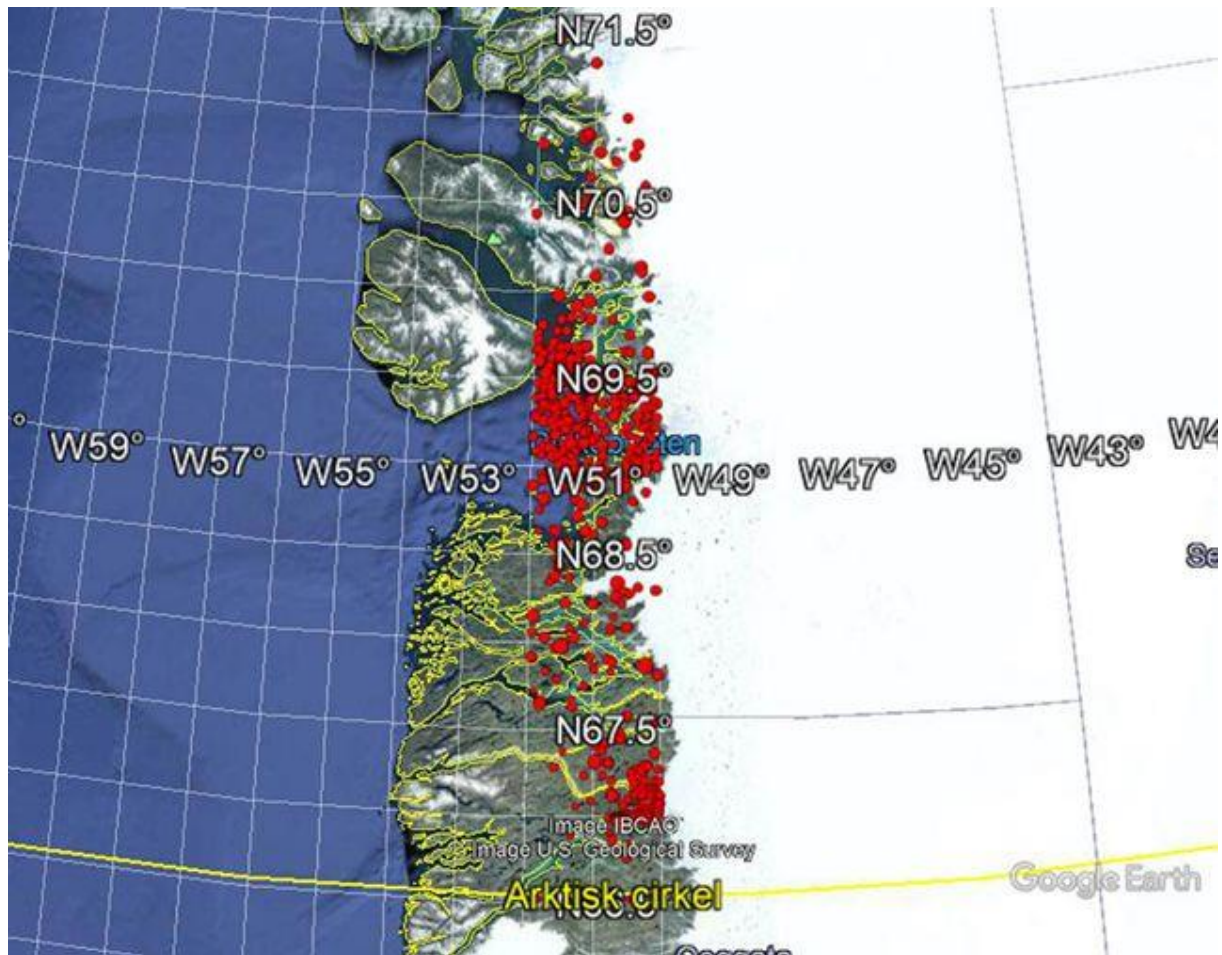


Figure 4: Map of Western Greenland with earthquake epicenters given by red circles.

We extracted the earthquakes from the web service in Nordic format and added the data to a SEISAN database (Havskov et al., 2020). We thereafter used the statistical tool within SEISAN to compute the distribution of earthquakes as a function of magnitude. From the distribution, we estimated the a and b values, see Figure 5:

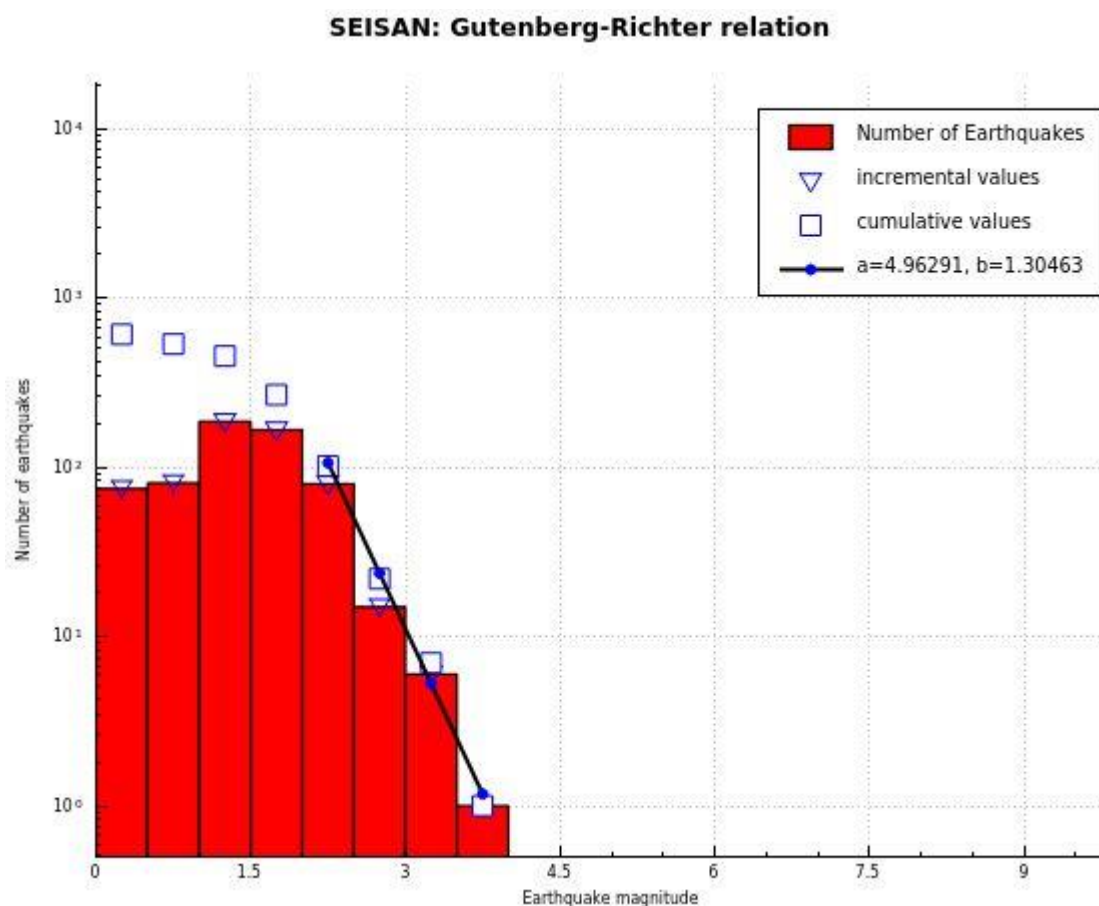


Figure 5: The a value represents the seismicity level in the area and the b values represent the magnitude frequency.

From the distribution of earthquake magnitudes in the Gutenberg-Richter plot in Figure 5, we derive the a value representing the seismicity level in the area and the b value representing the distribution of magnitude frequencies. The seismicity level and the magnitude frequencies in a region are important parameters in a probabilistic seismic hazard analysis (PSHA) procedure (Cornell, 1968). Extracting a and b values for areas of interest from the iAOS dataset will, when combined with an estimate of the maximum expected magnitude and knowledge on the attenuation of the seismic waves in these areas, provide the information needed for future PSHA in the arctic regions.

4.3. Mass loss from ice sheets and glaciers

Mass loss from glaciers and ice sheets impacts through the input of freshwater to the oceans on both local and global scales, and mass-neutral rainfall events impact the local oceans. We have generated multiple data products quantifying the solid mass loss, liquid mass loss, and rain runoff. We have also developed tools to improve the error estimates of the outputs to the ocean in the form of solid ice discharge.

Total mass loss is usually estimated from three different methods - volume change, direct measurements of mass change from the gravity field, or subtracting the outputs (surface, marine, and basal mass losses) from the inputs (e.g. snowfall). Here we apply the two latter methods to calculate time series of ice sheet mass loss.

Process understanding is key for improving projections of ice mass loss and its impact on the climate system. We have addressed this aspect in several studies focusing on the development of a method to separate mass loss from marine terminating glaciers into solid and liquid mass loss and how to estimate associated errors.

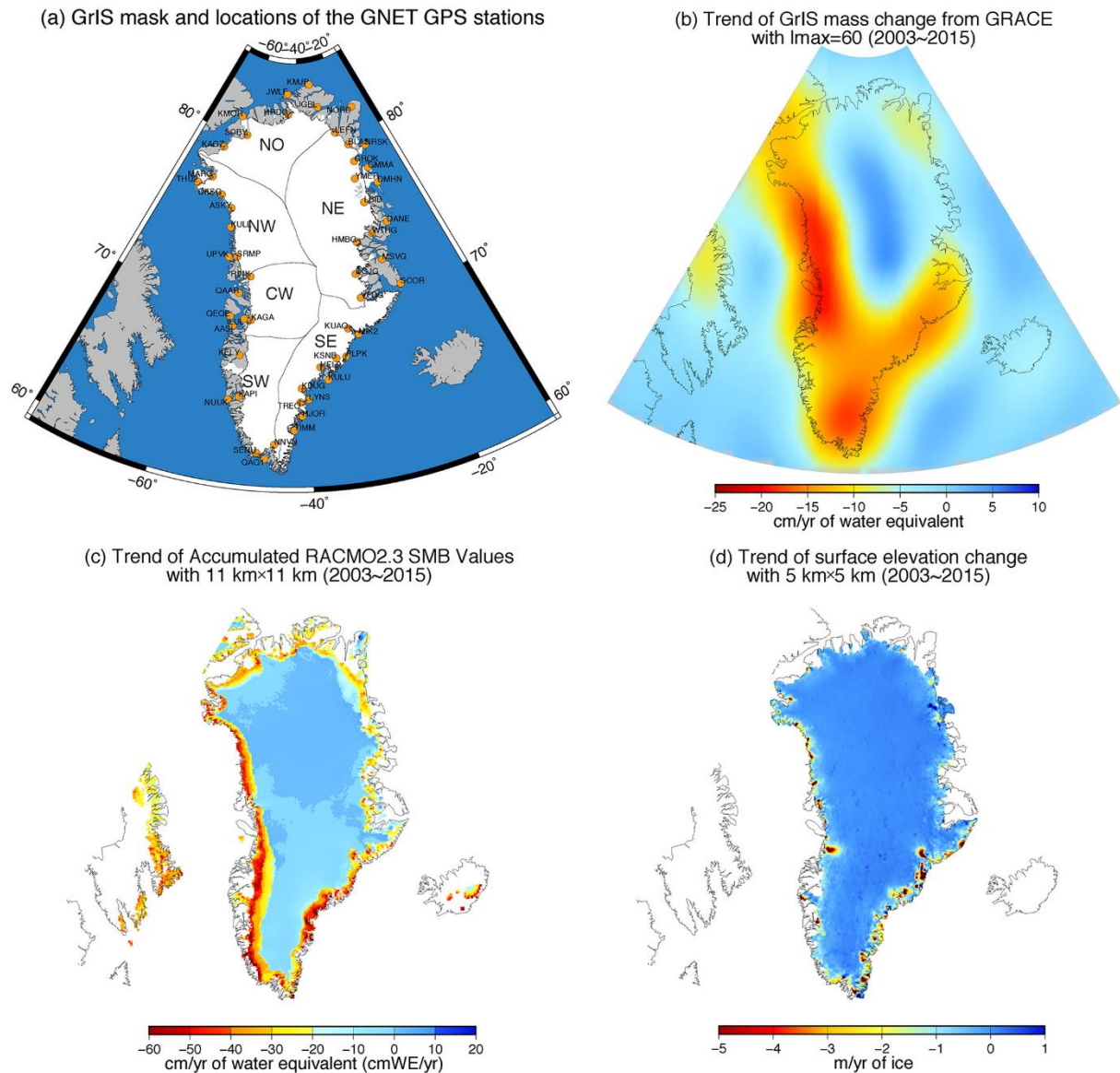


Figure 6: (a) Locations of the GNET stations shown by orange dots, (b) GRACE-derived linear trend of the GrIS mass change, (c) trend of monthly accumulated surface mass balance (SMB) anomalies, and (d) yearly surface elevation change (SEC) from 2003 to 2015. Black curves delineate major drainage basins according Rignot et al. (2011), with six subregions labeled as NE: northeast, NO: north, NW: northwest, CW: central west, SW: southwest, and SE: southeast.

4.3.1. Sea level: Mass change

Improved ice mass loss from satellite gravimetry

We have created a high spatial and temporal resolution ice sheet wide mass loss estimates using the GRACE satellite mission data. The coarse resolution estimates of the mass change derived from GRACE (Figure 6b) have been enhanced by the introduction of heuristic scaling factors applied to model surface mass balance (Figure 6c) and observed surface elevation change (Figure 6d). Corresponding results indicate large spatial heterogeneity in the gridded scaling factors at the $0.5^\circ \times 0.5^\circ$ scale, reflecting significant mass losses concentrated along the ice sheet margin and relatively small internal ice sheet changes at higher elevations.

However, this mass-change method does not support attribution of the changes - that is, GRACE does not know whether the changes in ice mass is caused by changes in snowfall, surface melting, or discharge.

The new enhanced dataset combined with GNET (Figure 6a) uplift data improve the spatial resolution and pinpoint areas of potential risk for large earthquakes. Based on ice mass loss, we have created maps of elastic deformations of the earth's crust and validated results with observations from the GNET network.

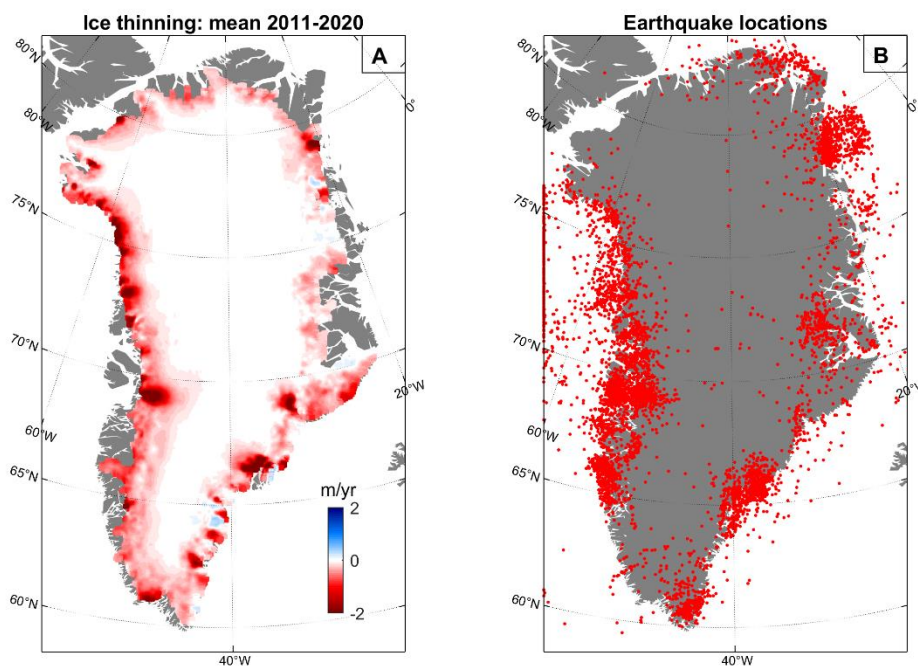


Figure 7: (A) Mean elevation change rate of ice surface during 2011-2020. (B) Location of all resisted earthquakes from 1972 to 2020.

Improved elevation changes from satellite altimetry

Figure 7a shows the average 2011-2020 mass loss, which is highly variable from year to year (as shown in Figure 8), while Figure 7b shows all seismic events detected during 1972-2021. There seems to be a correlation between mass loss and location of earthquakes.

Previous altimetry studies used observations from one satellite mission or fusion of multi-sensors to estimate trends over various time intervals, typically between 5-10 years (Csatho et al., 2014; Smith et al., 2019; Gardner et al., 2013; Sørensen et al., 2018). A small number of studies provide annual elevation change estimates, e.g. on spatial resolution of 5 km (Simonsen et al., 2021) and some use a 5-year running mean to estimate annual changes (Sørensen et al., 2018). Several methods have been used to estimate ice sheet surface elevation changes, e.g. orbit crossing points, along repeated ground tracks or using plane-fit solutions (Sørensen et al., 2011; Hurkmans et al., 2014; Khan et al., 2014). Here, we use a method similar to Csatho et al. (2014) but with modifications to estimate annual mass changes of the Greenland Ice Sheet on a high resolution (1x1 km) grid. Using the high spatial and temporal resolution grid, we are able to examine the complex evolving regional variations in mass loss, driven by both SMB and ice dynamics.

Our new product of high spatial resolution (1x1 km) and high temporal resolution (annual) elevation change rates covering the GrIS are shown in Figure 8 and may be used for further ice sheet mass loss - earthquake investigation and natural hazard assessment in the Arctic.

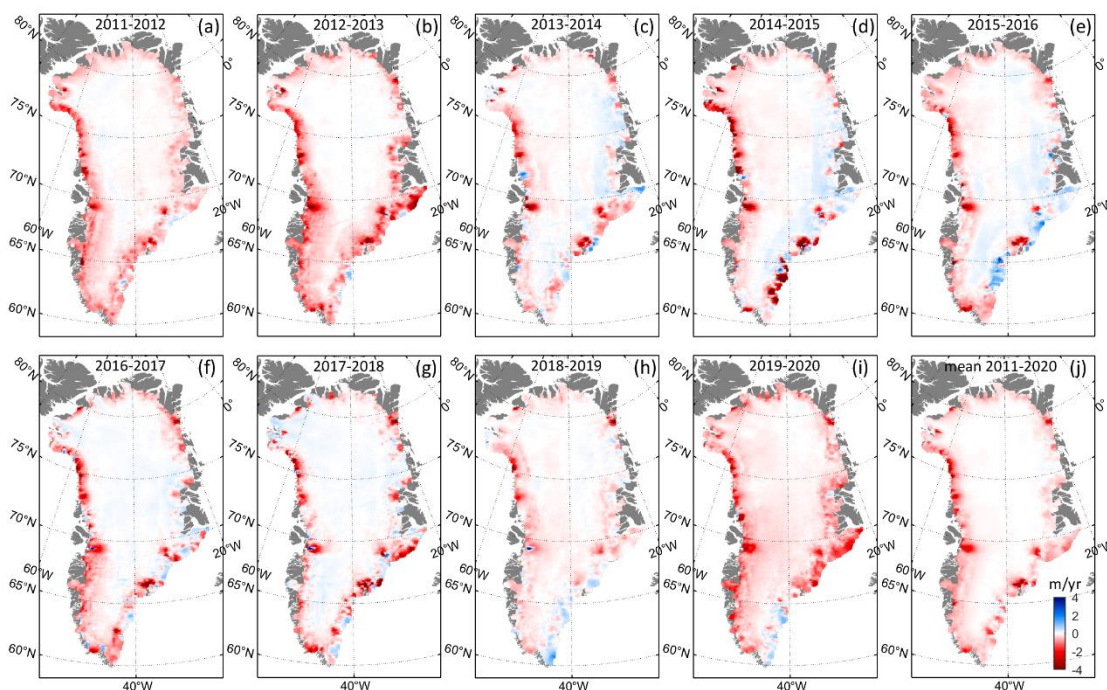


Figure 8: (a-i) Annual (April to April) elevation change rates of the GrIS from April 2011 to April 2020 from CryoSat-2, ICESat-2 and NASA's ATM flights. (j) mean elevation change rate from April 2011 to April 2020.

4.3.2. Sea level: Input/output

The input-output (IO) method is an alternate method for estimating the total mass balance. It compares favorably with the GRACE mass change estimate, but allows process attribution because the inputs and outputs, each composed of several terms, can be examined.

A work-in-progress uses regional climate models (RCMs), solid ice discharge, and basal mass balance, to estimate the IO mass balance. We use the HIRHAM/HARMONIE (Christensen et al., 2006), MAR (Fettweis et al. 2020), and RACMO (Noël et al. 2018) RCM surface mass gain terms, the same three RCM surface mass loss terms (combined as surface mass balance or SMB), a solid ice discharge product for the marine mass balance (MMB) term (Mankoff et al. 2020; described below), and a new data product (Karlsson, 2021) for the basal mass balance (BMB) term. The mass balance is then computed as $MB = SMB - MMB - BMB$.

4.3.3. Solid ice discharge

We have created a high spatial (glacier scale) and temporal (bi-weekly) estimate of where and when solid ice and submarine melt discharges into the surrounding fjords and seas (Figure 9). This is an “operational” product from 1968 until last month, updating approximately every 12 days with a one-month lag. Discharge is provided for every marine terminating outlet glacier. The product is described in detail in Mankoff et al, 2020a and is available through the INTAROS dataportal and the GEUS dataverse repository (https://dataverse01.geus.dk/dataverse/ice_discharge).

Inputs to this product are the PROMICE Sentinel Ice Velocity product (Solgaard et al 2021; in review) which can be accessed through the INTAROS catalogue, and the BedMachine dataset (Morlighem et al., 2017) for ice thickness. From these two products, ice volume flow rate across flux gates is computed as velocity times ice thickness times gate width times ice density (Figure 11).

This solid ice discharge is either submarine melt (which impacts ecosystems as described in the Freshwater Runoff section below), or icebergs, which are both an important part of the Greenlandic tourism economy, a navigation hazard for boats and ships, and a potential tsunami-source hazard for coastal towns (in 2018, a large iceberg near Innaarsuit made international news as a tsunami hazard).

Ice discharge uncertainty is ~10 %, due primarily to uncertainty in the ice thickness. As the ice thickness product (BedMachine) is updated with community inputs from additional borehole and radar flight lines, this uncertainty will decrease.

The following section (Section 4.3.4) provides a thorough description and analysis of how to estimate the error, when calculating solid ice discharge. A description of how the errors are estimated specifically for the solid ice discharge product described in this section is given in Mankoff et al, 2020a.

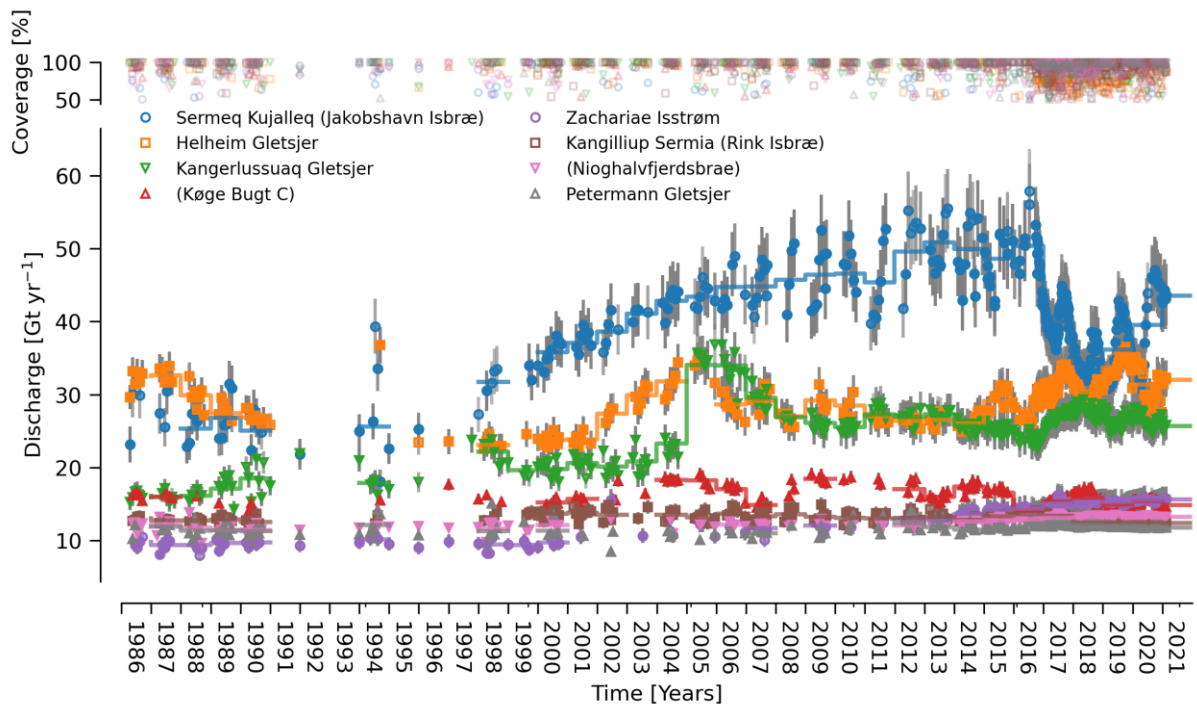


Figure 9: Discharge time series for eight major glaciers.

4.3.4. Error estimates for solid ice discharge to the ocean

Frontal ablation, that is, mass loss by calving, subaerial frontal melting and sublimation and subaqueous frontal melting Figure 10, is an important component of the mass balance of tidewater glaciers and marine-terminating ice caps. It has been reported to account for up to 30-50% of the total ablation of some Arctic glacierized archipelagos and ice caps (Dowdeswell et al., 2008; Sánchez-Gómez et al., 2019).

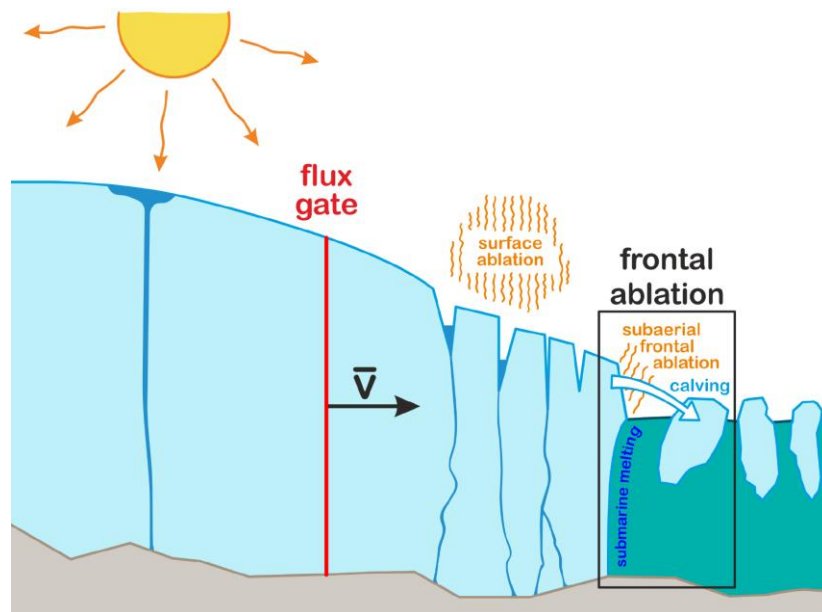


Figure 10: Components of frontal ablation. Subaerial frontal ablation is often negligible as compared to the other components.

Because of the difficulty of calculating separately the components of frontal ablation, it is usually approximated by the solid ice discharge through flux gates close to the calving fronts, calculated as the product of density, ice velocity and cross-sectional area (mass flux per unit time) (Figure 11). Ice surface velocity is usually obtained from satellite Synthetic Aperture Radar (SAR) data and ice-thickness from airborne ground-penetrating radar (GPR) data. If the considered flux gate is not close to the calving front, the surface mass balance between them should be taken into account (Figure 10) - it is not in the solid ice discharge product described above (Section 4.3.3), because flux gates are placed only 5 km upstream from the termini. Possible front position changes and ice-thickness changes should also be taken into consideration. The former, because a change in front position (assuming a fixed-location flux gate) makes different frontal ablation and ice-discharge through the flux gate, and the latter because it implies a change in the cross-sectional and hence the flux across the gate.

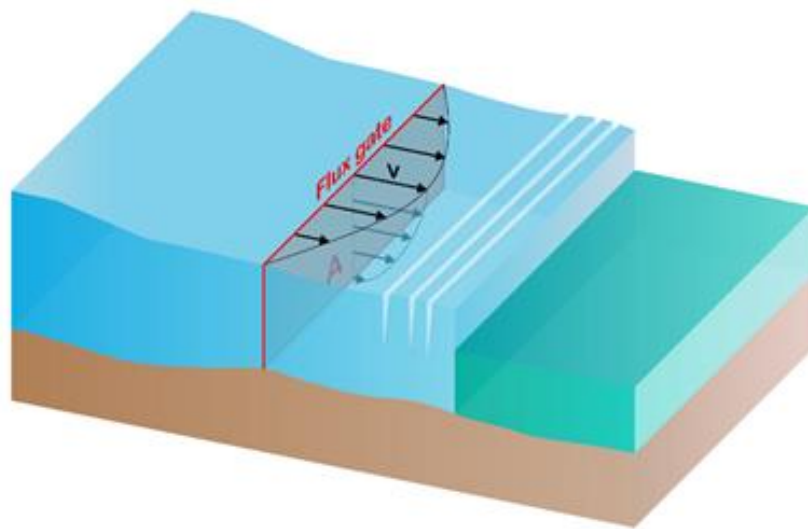


Figure 11: Solid ice discharge through a flux gate.

An important aspect of the ice discharge estimates is the quantification of the errors involved in its calculation. The usual error estimates for ice discharge are often based on rough estimates of upper and lower bounds for the error, rather than doing a statistical error analysis based on error propagation. Within INTAROS we have developed tools, based on statistical error propagation techniques, to estimate the error in ice discharge as a function of the errors in the variables and parameters involved in the discharge computation. Yet, some of these variables can be even unknown. In particular, the cross-sectional area of tidewater glaciers is quite often unknown. For many tidewater glaciers, sometimes only ice-thickness profiles along a central flowline are available (usually from airborne radar sounding data), which means that the ice thickness is only known at a single point at the glacier front (and assumed to be small at the contacts with the glacier walls). In such cases, U-shaped cross-sectional area approaches are often used, but the errors involved are large and their estimates frequently rely on simplistic assumptions. We have also developed improved tools to address this problem. All of these studies have been compiled in Sánchez-Gómez and Navarro (2018) and are summarized below.

As mentioned, ice discharge is calculated as mass flux per unit time across a given vertical surface S , approximated using area bins as

$$\phi = \int_S \rho \mathbf{v} \cdot d\mathbf{S} = \sum_{i=1}^n \rho L_i H_i f v_i \sin \alpha_i$$

where the variables in the right-hand side of the equation are, respectively ice density, the length and height of each area bin, the conversion factor from surface velocity to vertically-averaged velocity, the surface velocity and the angle between the glacier velocity vector and the vector normal to the cross-section used for the flux calculation.

Therefore, for glaciers with available GPR cross-sectional profiles, the total error in ice discharge can be calculated, using error propagation, as

$$\sigma_\phi = \sqrt{\sigma_{\phi_\rho}^2 + \sigma_{\phi_H}^2 + \sigma_{\phi_f}^2 + \sigma_{\phi_v}^2 + \sigma_{\phi_\alpha}^2}$$

where the various quadratic terms represent the contributions to the error due to the uncertainties in the corresponding variables or parameters. There is no error term for L as this is assumed to be error-free. The error term for f is often small. Each of the above terms is of the form (taking one of them as an example):

$$\sigma_{\phi_H} = \sqrt{\sum_i (\sigma_H \rho L_i f v_i \sin \alpha_i)^2}$$

The analysis in Sánchez-Gómez and Navarro (2018) shows that the velocity field is the dominant source of error for small glaciers with low velocities, while for large glaciers with high velocities the error in cross-sectional area becomes the main contributor to the total error. This finding stresses the interest of measuring ground-penetrating radar (GPR) cross-sectional profiles for the largest glaciers. They have also shown that glacier thinning/thickening between the times of SAR and GPR data acquisitions should not be disregarded, as it can imply a bias in the ice discharge estimate of up to $\pm 8\%$ for their case study, encompassing many Canadian Arctic glaciers.

For the case in which GPR ice-thickness profiles are only available along (or close to) the central flowline of the glacier, we have developed a method to estimate the error in ice discharge when various U-shaped cross-sectional approaches are used (Figure 12, left panel). As shown in Sánchez-Gómez and Navarro (2018), the parabolic approach allowing for the axis of the parabola to be displaced with respect to the GPR flight line (Figure 12, right panel) generally performs better (low bias and admissible standard deviation) than the axis-centered parabolic approach usually employed in the literature. Finally, we have also developed a method to choose the optimal location of the U-shaped cross-section in terms of the along-flow variations of ice discharge, surface velocity and ice thickness. The details can be found in Sánchez-Gómez and Navarro (2018).

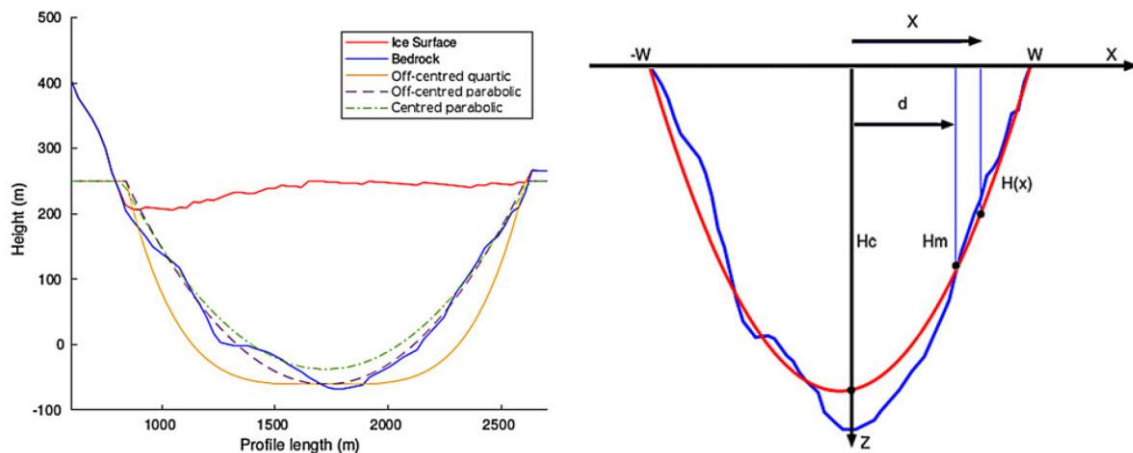


Figure 12: Left: Various cross-sectional U-shaped approaches. Right: Parabolic approach allowing for axis of parabola displaced with respect to the GPR flight line by an amount d (from Sánchez-Gómez and Navarro, 2018, figs. 1b and 2, respectively)

4.3.5. Partitioning of ice discharge into iceberg calving and submarine melting

We have developed a model-based approach to separate the frontal ablation of tidewater glaciers (or, equivalently, ice discharge, if a flux gate close to the calving front and a stable glacier front position are assumed) into its two main components, iceberg calving and submarine melting (Figure 10). In fact, we have developed two separate approaches:

- One of them (De Andrés et al., 2018) is based on a coupled glacier dynamics-fjord circulation model. It is the most complete approach, but it is computationally expensive.
- The second approach (De Andrés et al., 2021), substantially less computationally expensive, couples a glacier dynamics model (Otero et al., 2017) with a plume parameterization model (De Andrés et al., 2020).

We briefly review here both models, which are developed in detail in Deliverable D6.17.

Coupled glacier dynamics-fjord circulation model

Glacier dynamics model. The glacier dynamics model uses the software Elmer/Ice to solve, using finite element methods, the Stokes problem governing glacier dynamics. The Stokes system of equations encompasses the equations for conservation of mass and linear momentum, which are complemented by a nonlinear constitutive equation, namely Nye's generalization of Glen's flow law. We introduce a scalar damage variable to account for fracture-induced softening of glacier ice. As the model is two-dimensional, a body force term is added to the equation of conservation of linear momentum to account for friction from the shear margins. The time evolution of the glacier surface is calculated by solving the free-surface evolution equation that takes into account the flow of ice and the surface mass balance. The glacier model incorporates a calving submodel, based on crevasse-depth penetration, which assumes that calving is triggered by the downward propagation of transverse surface crevasses occurring near the calving front as a result of the extensional stress regime (Otero et al., 2017).

The model requires as input data the glacier geometry (upper surface and bed geometry, and calving front position), surface velocities, surface mass balance and ice-melange coverage (the latter, to estimate the backstress exerted by the ice-melange on the glacier front). The model generates as output the velocity and pressure fields across the glacier, from which all components of strains and stresses can be derived. The evolving geometry of the glacier surface and the front position changes are also derived from the model output, as well as the detachment of portions of the glacier front by calving processes.

Fjord circulation and submarine melt models. The fjord circulation model, in turn, uses MITgcm software to solve, using the finite volume method, the Navier-Stokes system of differential equations (with the Boussinesq approximation) governing the fjord circulation. The equations driving the fluid dynamics are those of conservation of mass, momentum, heat and salt. Density of seawater is defined as a function of temperature and salinity by means of a non-linear equation of state. The 2-D configuration of the model is partially compensated by a proper choice of the viscous and diffusive coefficient values. The fjord circulation model is completed by the Holland and Jenkins equations defining the thermodynamic equilibrium (salt and heat balance) at the fjord-glacier front interface, which allows computing the melt rate of ice at the glacier-fjord interface (De Andrés et al., 2018).

The fjord circulation and submarine melt models require as input data the fjord bathymetry, the subglacial discharge rates, and water temperature and salinity data from CTDs. The model generates as output the evolving velocity, temperature, salinity and pressure fields across the fjord and, most importantly for our purposes, the melt rates at the glacier front (as a function of depth).

Coupling between models. Coupling between the glacier and fjord models (Figure 13) is accomplished through two main mechanisms: 1) the depth-dependent submarine melt rates modify the shape of the submerged part of the glacier front, resulting in a new glacier model domain, which in turn implies changes in the stress regime; and 2) the front position changes derived from the glacier dynamics model modify the fjord domain length and thus the fjord water circulation regime.

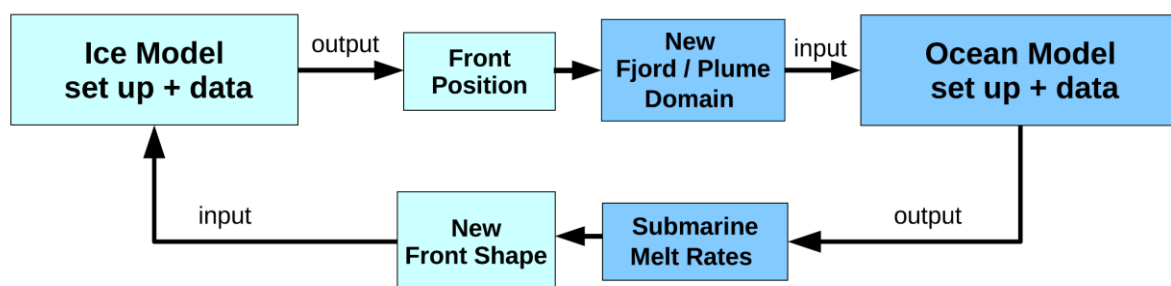


Figure 13: Workflow diagram of the coupled model. The ocean model here represents either component, the line-plume or the fjord circulation model (from De Andrés et al., 2021, Fig. 3).

Coupled glacier dynamics-plume parameterization model

The glacier dynamics model is exactly as in the above case, but the fjord circulation model, which is the most computationally-expensive part of the coupled model, is replaced by a parameterization of the buoyant plume, as described below.

Buoyant plume model. The buoyant plume model is based on the line-plume model of Jenkins (2011) slightly modified by Slater et al. (2016) to allow the calculation of plume properties beyond its neutral buoyancy and up to its maximum height. This model is steady in time and the only independent variable for tidewater glaciers is the vertical dimension, so it is strictly a 1-D model that considers constant plume properties along the plume width. The evolution of the plume properties (thickness, vertical velocity, temperature and salinity) along the vertical tidewater face is described by four ordinary differential equations describing the conservation of the fluxes of mass, momentum, heat and salt. The plume model is closed using a thermodynamical equation of state to calculate the plume and ambient (fjord water) densities and the submarine melt rates using the same melt model as described above (De Andrés et al., 2020, 2021).

Comparing the performance of both coupled models (De Andrés et al., 2021)

Applied to Hansbreen-Hansbutka glacier-fjord system, in southern Svalbard, both coupled models (glacier-fjord and glacier-plume) predicted observed front positions reasonably well (± 10 m) when using the best-fit configurations for the parameters of subglacial discharge intensity and crevasse water depth (both of which influence calving rates). Although the two models showed different melt-undercutting front shapes, which affected the net-stress fields near the glacier front, no significant differences of the simulated glacier front positions were found. In terms of frontal ablation partitioning, both models showed that cumulative submarine melting is equivalent to cumulative calving to the end of the melting season. Regarding computational cost, the glacier dynamics-line plume model was 50 times computationally faster than the glacier dynamics-fjord circulation model.

Further details on both models can be found in Deliverable D6.17, which is a demonstration for stakeholders on how the integrated Arctic Observation System (iAOS) can be used to retrieve the ice discharge from glaciers to the ocean and how the above models can be used to separate the frontal ablation into its two main components, glacier calving and frontal submarine melting.

4.3.6. Freshwater runoff

The above terms are directly related to mass loss, but an additional product has been generated - freshwater runoff (Figure 14). This includes melted ice (a mass loss term) but also rainfall which is mass neutral. We have created a high spatial (outlet scale) and temporal (daily) estimate of where and when liquid freshwater (i.e. rainfall, melted ice, and melted snow) discharges into the surrounding fjords and seas from 1958 through 2019. This product is generated from the HIRHAM (Langen et al. 2017) and MAR (Fettweis et al, 2020) RCMs and the ArcticDEM surface topography (Porter et al. 2018). The freshwater runoff product captures flood event hazards (for example the 2012 Kangerlussuaq river overflow event that destroyed the bridge), in addition to the seasonal cycle, and changes in baseline runoff over the study period. The freshwater product is described in Mankoff et al, 2020b and it can be accessed through the INTAROS datportal and is stored in the GEUS dataverse repository (<https://dataverse01.geus.dk/dataverse/freshwater>).

With this product quantifying liquid water runoff, stakeholders now have access to a dataset that can be used for a variety of ecosystem model studies related to the regional fishery economy or safety and hazards.

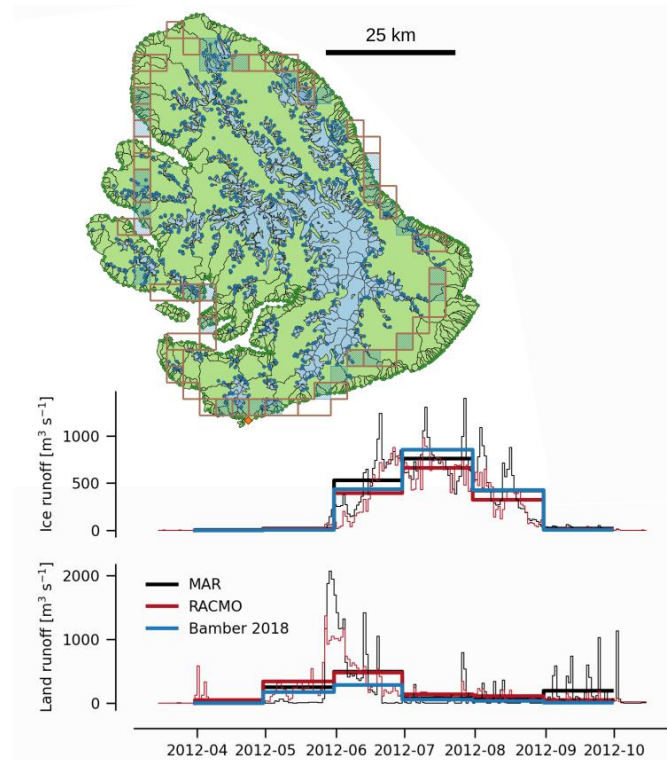


Figure 14: Example of freshwater discharge product. 100 m ice basins (blue lines) and outlets (blue dots) and land basins and outlets (green lines and dots respectively) cover Disko Island. Each outlet has a runoff time series, but the entire island runoff (summed) is shown below for ice (upper graph) and land (lower graph).

5. Synthesis on achievements concerning stakeholder needs and data gaps

In this section we discuss how well the results from Task 6.4 (described in Chapter 4) using data and methods from the iAOS fulfill the needs of the stakeholders. Are we closing gaps and are new sensors or other types of data required in an improved/future iAOS?

5.1. Snow avalanche

The demonstration on how to utilize in-situ snow and meteorological variables to improve the input to snow models used for avalanche forecasts (e.g. SNOWPACK, CROCUS) showed that indeed near surface wind (direction and speed) can be utilized as a predictor for snow erosion/accumulation along the analyzed mountain slope. However, longer time series of collocated snow and meteorological observations from the snow release areas around Longyearbyen would be needed to develop a more robust methodology. The discontinuity of the current in-situ snow datasets due to changes in location of the stations and in the applied instrumentation, the large temporal gaps, and the lack of collocated wind measurements pose strong limitations to the use of the data for snow model development and improvement of avalanche forecasts.

The geostatistical package applied to produce the high resolution gridded map of snow depth in the Longyeardalen valley demonstrated to be a potentially powerful tool to extrapolate the sparse, station-based snow observations to a wide gridded area with high (25 m) spatial resolution.

Weather forecast models still have too coarse spatial resolution to produce near surface wind and precipitation that would be precise enough for snow avalanche prediction models. Forecasted snow accumulation can be empirically corrected based on in-situ observations. However, to make a more detailed statistical correction of snow depth, longer time series of collocated snow and meteorological observations from the snow release areas around Longyearbyen would be very much needed. Terrestrial laser scanner (TLS) would provide invaluable data of the snow thickness distribution at the slopes surrounding Longyearbyen. TLS data could also allow us to determine over which areas the pointwise corrections can be generalized. Meteorological, snow depth, and TLS data collections should be fully automatic to enable real time data delivery.

5.2. Earthquake, landslide, tsunami

In terms of providing new knowledge on seismic activity in the Arctic region, both the OBS and the CBM deployments have fulfilled the needs in the areas of deployment. The data have provided new observations on seismic activity previously unknown and additional information on seismic events improving their location in space and time. These observations will improve the accuracy of future investigations of e.g. earthquake hazard.

For future monitoring of events with a seismic signature, such as earthquakes, landslides and tsunamis, the quality of collected data has provided useful information to stakeholders that will guide the quality assurance process for future deployments.

Both the OBS deployments in the North Atlantic Ocean and the CBM in the Disco Bay area, Greenland, have closed gaps in the seismic observation of these regions, during the time of deployments.

For an improved future iAOS, additional data are required in order to provide knowledge beyond spatial and temporal location of seismic events. The mechanisms that release the seismic events, such as the stress induced by plate tectonics, are only well understood for larger earthquakes (magnitude 5+), based on the permanent monitoring. For smaller earthquakes and other seismic events, a denser, long-term monitoring is needed. This requires access to power and communication. In coastal regions, this can be obtained using existing technology, but power supply and internet access is challenging at remote locations, especially in the ocean. In addition to cabled OBS deployment, long-term seismic monitoring on the sea bottom can be achieved with other types of cabled systems, allowing for continuous power supply and real time data transfer. Fiber-optic cables have been demonstrated as potential seismic sensors, also in remote/inaccessible areas. Floating seismometers (Mermaid systems) may be another solution for seismic monitoring, potentially also under the sea ice, if the technology is further developed. Effort should be put into multi-hazard and -risk assessment in the arctic region, considering the effects of climate change and also the potential for cascading events. Such effort should allocate sufficient resources to visualization and provision of data to relevant stakeholders.

5.3. Mass loss from ice sheets and glaciers

Stakeholder needs: Both the solid ice discharge and freshwater runoff products are provided at high temporal and spatial resolution, are freely available and the solid ice product is updated continuously. The products are stored in a Dataverse repository, have a DOI and are described thoroughly in the data journal Earth System Science Data (ESSD). This makes the products easier to use, as they have undergone a peer review quality assessment. Both products have a GitHub page where users can post issues, make suggestions, or ask questions relating to the products. For the freshwater product, the GitHub page includes scripts facilitating use of the data. Furthermore, the freshwater runoff is provided as part of the hydrology layer in QGreenland (<https://qgreenland.org/>) promoting it to new users and making it easier to synergize with other products. It is important to make stakeholders (researchers/users) aware that these products exist for them to be purposeful and be of use to stakeholders further downstream.

The method to estimate the error in ice discharge as a function of the errors in the various data sources involved in ice discharge computation (ice thickness, ice surface velocities, conversion factor from surface velocities to column-averaged velocities, ice density, etc.) has been developed and published in an open-access journal (Sánchez-Gómez and Navarro, 2018) so it is freely and easily available. Given that this is a methodological paper, although the application shown in the paper corresponds to Arctic Canadian glaciers, the method can be applied to any region. The only limitation is that the method has been developed for tidewater glaciers, so it would need some extension for the case of ice shelves or glaciers with floating tongues, even if these are very scarce in the Arctic region.

A similar comment applies to the method to separate the two main components of ice discharge (iceberg calving and submarine melting). The method has been published in a set of three closely related papers (De Andrés et al., 2018, 2020, 2021), all published in open-access journals. In this case, the glaciers used to test the method are located either in Svalbard (first and last references) or Greenland (second reference). Once again, as the papers are aimed at process understanding, the knowledge gained on such processes can be extrapolated to any Arctic glacier of similar characteristics. The main limitation here is that the model developed under INTAROS is two-dimensional. Although some mechanisms have been introduced to account for 3-D effects (e.g. the effects on dynamics at the glacier central flowline by friction at the lateral glacier walls, or the simulation of discharge channels distributed along the actual 3-D tidewater calving front into a 2-D model), other effects are not properly accounted for. This affects in particular the simulation of the fjord circulation and its effects on the submarine melt rates at the glacier front. Only a full 3-D model could properly account for these processes. Although UPM is already working on it, we do not expect any significant results before the end of the INTAROS project.

A GNET website is under construction and processed data, time series of 3D crustal displacements will be available from 2021. The time series will be updated daily and consist of daily solutions of crustal displacements. The goal is to provide real time monitoring of local ice mass loss for each sector of the Greenland ice sheet. For example, a warm summer with a large melt will immediately be detected as perturbations in uplift. For ice sheet-wide mass loss, GRACE and GRACE-FO, do not fulfill the needs of the stakeholders. The resolution of the improved data set provided here is still not good enough to study individual glaciers.

Closing Gaps: The freshwater runoff product has closed an important gap to ecosystem model studies (related e.g. to regional fishery) by providing a high spatial (outlet scale) and temporal (daily) estimate of liquid freshwater discharge (from rainfall and from ice and snow melting) into the surrounding fjords and seas. Similarly, the ice discharge product has closed a relevant gap in estimating how the total mass balance of the Greenland ice sheet separates into solid ice discharge and surface mass balance, which is of great interest for understanding and forecasting the response of the ice sheet to climate changes. In this case, this has been achieved by providing a high spatial (glacier scale) and temporal (bi-weekly) estimate of solid ice and submarine melt discharges into the surrounding fjords and seas.

The method to separate ice discharge into iceberg calving and submarine melting, in turn, has contributed to closing the gap in understanding the partitioning of ice discharge into its two main components. This, again, is fundamental to the model-based estimates of the future evolution of the Greenland Ice Sheet. Finally, the method to estimate the error in ice discharge as a function of the errors in its various input data sources has filled a significant gap in the uncertainty estimates associated with ice discharge computations, by narrowing their error ranges.

Regarding mass loss observed by GRACE and GRACE-FO we are working on closing the gaps, and a new method to estimate ice discharge using GNSS time series is being developed (Hansen et al., 2021, in review). Dynamic thinning is typically largest near the glacier terminus and along the main flow-line and declines rapidly inland (Khazendar et al., 2019), while SMB-induced thinning has a much larger wavelength as SMB anomalies typically have a larger footprint. Earth's elastic response due to dynamic thinning can be isolated by applying a correction for SMB-induced elastic uplift. Therefore, a GNSS station located near a glacier front can sense and reveal the dynamic mass changes of that particular glacier. The major advantage of using GNSS data is the very high temporal resolution (daily) of elastic uplift estimates, caused by daily mass loss variability of the nearby glacier. We are in the process of developing parameters that can convert uplift measured in mm/yr to discharge measured in Gigaton/yr. Such parameters will close the gap and provide high-resolution discharge time series.

Improvements: The daily resolution of the freshwater runoff product introduces significant errors and uncertainty that require further work. Specifically, stream dynamics must be incorporated into this work in order to properly capture the time lag between when a parcel of water melts far inland on the ice sheet and when it is discharged through the outlet point into the fjord. Currently, transport is instantaneous, so although the product is available at daily resolution, long temporal averaging is required to reduce the signal to noise ratio. It is important for high temporal resolution studies that we improve the quality of the daily product.

Both the solid ice discharge and freshwater runoff products rely on maps of bedrock to determine the ice thickness at the individual flux gates and to determine the water routing. Even state-of-the-art bedrock datasets have high uncertainties, because a large part of the ice sheet bedrock has not been surveyed or is located in regions where water hampers the measurements. This introduces further errors to derived products like the solid ice discharge and freshwater runoff.

Ice velocity maps derived from SAR data often have gaps over large regions in summertime due to surface melt. For products like the solid ice discharge this means that periods with high speeds are not captured properly. Better ice velocity maps during summer can be achieved by merging ice velocity derived from both optical and SAR sensors.

Currently, no operational high-spatial and high-temporal resolution of MB exists for Greenland. This is needed to estimate individual basin-scale and synoptic-scale mass balance change events.

The solid ice discharge product and freshwater runoff products are limited to Greenland. It would be of interest that similar products were developed for Svalbard, for which the data availability is scarcer and dispersed among various data sources.

The method to separate ice discharge into iceberg calving and submarine melting requires, as described in sections 3.4 and 4.3.5, plenty of data from the glacier, fjord waters and overlying atmosphere environments. Because the method is mostly aimed at process understanding, such data are only needed for selected glaciers. However, it often happens that a given glacier has plenty of glaciological and atmospheric/radiation data but lacks the necessary fjord waters data. Conversely, for some glacier-fjord systems many oceanographic measurements are available, but the glaciological data is scarce. Therefore, it would be of interest to define some supersites where all sets of data were available. This could be achieved by promoting that new glaciological programmes or oceanographic deployments were undertaken not at new sites but at sites for which the planned data acquisitions could complement already existing data. This point will be further discussed in Section 6.

The amount of GNSS sites is limited and the recently developed tools to monitor ice discharge of individual glaciers using GNSS are limited to 5-10 glaciers. Though the network consists of more than 64 sites, the location is not optimal for mass loss estimation. Therefore, relocation of sites or installation of new sites is recommended.

6. Recommendations to Roadmap

In INTAROS task 6.4 we have addressed three natural hazards in the Arctic using data and tools available through the iAOS. Although Arctic natural hazards are not limited to these three, their diverse nature illustrates well the key issues related to providing the necessary hazard information to stakeholders. Based upon the work we have carried out in this task, we discuss general, overarching themes relating to tending to stakeholder needs and further development of methods and monitoring services.

6.1. Long time series

Long time series of observations are a key point to all hazard studies in INTAROS task 6.4. The work of downscaling RCM-output of snow depth was difficult due to the lack of observations. In this example, time series of collocated in-situ snow and meteorological data are needed to develop robust statistical methods to downscale the outputs from regional forecast models such as AROME-Arctic. The time series should cover several consecutive years, thus enabling the identification of relationships between the occurrence of heavy precipitations, large snow accumulations, and atmospheric observations.

Longer time series improves our process understanding which in turn will improve assessments and predictions. For the earthquake hazard, longer time series improves the knowledge of the spatial and temporal distributions of previous earthquakes, which is a key component in earthquake hazard assessment. For estimating the interannual variability of ice discharge and its two main components (iceberg calving and submarine melting), and how they respond to environmental changes, as well as for calibrating and validating the models allowing the partitioning of ice discharge into its two mentioned components, it is crucial to count with long time series of many types of glacier and fjord data, some of which can only be collected in-situ. The vast amount of input data required by such models makes this task infeasible, unless the modelling is restricted to particular supersites, as will be discussed in Section 6.4.

Validation of data products also require long, consistent observational time series. An example of this is the freshwater run-off product, which is based on RCM-output and elevation models. In this example, the river discharge observations like the one from the Watson River in west Greenland is one of the few available validation data sets. RCM results also require validation data to ensure the quality of results. For this, long term observations from automatic weather stations of multiple meteorological parameters are necessary.

6.2. Services in real time

Many operational services rely on input data to be available in real time or close to real time in order for authorities to be able to respond timely. In INTAROS task 6.4 this is the case for the avalanche and earthquake hazards. For operational snow avalanche forecasting, automatic snow and meteorological observations along the mountain valley where snow avalanches can occur and could cause damages should be transmitted to users in real time. In this way, the data can be used as input to the snow models used to forecast the risk of avalanches. For operational earthquake detection, real time data collection and data transfer enables a fast response to authorities and the public regarding large landslide/earthquake/tsunami events. Having data transmitted in real time also provides the possibility to catch if instruments fail or if data quality is lowered. Real time therefore enables fast instrumental replacement to prevent data gaps and low data quality

For other types of operational services, “real time” can also mean that input data is updated regularly, but on the scale of days or weeks. In task 6.4, the operational solid ice discharge product and mass balance product rely on ice velocity (and RCM) output to update regularly. It is crucial for the products that the input datasets update regularly, but even with a lag of weeks both products are useful for monitoring and for reuse by others. The key point being that the time series keep updating, which again points to the subsection above on the need for long time series.

6.3. Availability of datasets

In task 6.4, the results of the solid ice discharge and freshwater run-off products are freely hosted on the GEUS dataverse. Furthermore, these products have a GitHub page where users can post issues or ask questions. This benefits the data product as the feedback and resolved issues are documented.

Seismological data carrying vital information on hazardous events should be provided in real time to international databases to make better and more independent analyses. See e.g. the European EIDA system (e.g. The Norwegian EIDA node <https://eida.geo.uib.no/webdc3/>) or the IRIS initiative from the USA (<https://www.iris.edu/>).

We have also increased the visibility of the freshwater flux product by adding it to QGreenland. This is one way of increasing product visibility and providing access to users outside the glaciological community. Making datasets available and/or visible and usable to other scientists/experts/users with other backgrounds paves the way for more cross disciplinary research. Within task 6.4 the work presented in Svennevig et al. (2019, 2020a and 2020b) is an example of this. In the study, different kinds of satellite remote sensing techniques are combined with seismological observations to better discover and locate landslides in western Greenland. Freshwater flux data has been used as inputs for models of ocean physics, fjord biological systems, and human society impacts of fjord dynamics.

6.4. Super sites with multi-disciplinary observations

Studies of process understanding and the development of methods in many cases have difficulties due to lack of co-located observations. Often different types of data have been collected by different groups at different times making it difficult to study how processes co-evolve and affect each other over time.

A solution to this problem is to have super sites where multi-disciplinary observations are performed. We discuss this in the context of two examples from INTAROS task 6.4:

For the forecasting of hazardous events such as snow avalanches that are caused by the interaction of atmospheric and cryospheric processes, in situ stations collecting both atmospheric and cryospheric observations are needed. Our attempt to utilize in situ observations to constrain/downscale regional model output to improve snow avalanche forecasts in an area with complex topography clearly demonstrated that collocated, multidisciplinary observing approach is needed for the understanding and, thus, the modelling of the snow processes affected by the atmospheric forcings. This is especially the case in mountain regions where the spatial representativeness of snow and atmospheric observations can be extremely limited.

For process understanding, in particular regarding the partitioning of ice discharge into iceberg calving and submarine melting, plenty of in-situ data regarding both the glacier and the fjord systems, and their overlying atmosphere, are needed. These data are crucial for ground-truthing of remotely sensed data. Additionally, glaciological data are needed as input to the models of glacier dynamics, either as boundary conditions or to calibrate and validate the model results. Automatic weather station data are needed for downscaling of regional climate model results and to feed the models of melting at the glacier surface, which are in turn critical to estimate the subglacial discharge that enters the fjord system at the glacier grounding line through subglacial channels. Oceanographic data (currents, CTD) are needed to feed the models of fjord water circulation (or to constrain the buoyant plume parameterizations), either as boundary data (e.g. at the fjord mouth, to constrain the water inputs and outputs to/from the fjord) and/or to calibrate and validate the model results. As we have discussed in previous sections, some locations are rich in glaciological and meteorological data, while lacking oceanographic data, and conversely.

It would therefore be crucial to define some supersites, both in Greenland and in Svalbard, where the different types of observations mentioned were available. The easiest way to accomplish this would be that, rather than starting new programmes at locations with limited or no data, such new initiatives would focus on completing the lacking data (either glaciological/meteorological or oceanographic) at locations already counting with a dense set of observations but lacking data of certain types. This would require coordination between agencies at both the operational and funding levels.

A site currently close to such a status of supersite is the Hansbreen-Hansbutka glacier-fjord system in Hornsund, southern Svalbard. This is favoured by the location there, since the International Geophysical Year, of the Hornsund Polish Polar Station. The main deployment here would be some current meters at various depths at the fjord mouth, plus probably a more regular CTD monitoring in the vicinity of the glacier front.

Another suitable candidate in Svalbard could be the glacier-fjord system Kongsvegen/Kronebreen/Kongsbreen-Kongsfjorden, NW Spitsbergen, favoured in this case by the proximity of Ny Ålesund. Here, a stronger effort, in particular regarding oceanographic data, could be required.

In Greenland, regional climate, fjord geometry, ocean currents and outlet glacier depth and velocity vary widely, imposing limits to the representativeness of an individual supersite. In spite of this, supersites also represent the most promising avenue to understand the interconnected nature of the processes governing these systems in Greenland.

The Nuup Kangerlua/Kangiata Nunata Sermia (KNS) sub-Arctic fjord/glacier-system near Nuuk in Southwest Greenland is a strong candidate for a supersite, as many physical and ecological parameters are already measured in the fjord, atmosphere and cryosphere by existing monitoring programmes, namely the Greenland Ecosystem Monitoring (GEM) programme, Nuuk Basic, which covers the Kobbefjord Research Station for the terrestrial part and the fjord extending to KNS for the marine part, and the Programme for Monitoring the Greenland Ice Sheet (PROMICE), which covers ice sheet climate and surface melting from a neighbouring glacier to KNS, and ice velocity and discharge for the entire ice sheet margin. Challenges to turn this into an outlet glacier supersite include more hydrographic data near the glacier front, especially in the open water season, and continuous monitoring of the glacier front, including subglacial plumes and ice velocity.

Another candidate is Helheim Glacier in Southeast Greenland, which represents one of the largest outlet glaciers from the Greenland Ice Sheet in terms of ice flux, and is in the vicinity of both PROMICE stations on the ice sheet margin and the Sermilik Station at the fjord mouth. Challenges to turn this into a supersite include establishing continuous hydrographic measurements in the Sermilik Fjord, so far carried out in individual projects, and continuous observation of the glacier front for velocity, calving events and meltwater plumes. As with all the major ice streams from the Greenland Ice Sheet, the fjord near the glacier front is infested with a mixture of broken icebergs and remnant fjord ice (ice mélange) which constitutes a major obstacle for continuous measurements in the water.

In Northwest Greenland, Bowdoin Glacier near Qaanaaq has been monitored for nearly 10 years but would require a more comprehensive year-round monitoring to qualify as a supersite. Both Helheim and Bowdoin Glaciers are less comprehensive on the ecosystem aspect and both rely on annually recurring research projects and field campaigns.

Other large outlet glaciers from the Greenland Ice Sheet have been subjected to periodic supersite (or near supersite) status during major, but short-lived, research projects. However, the costly logistics of permanent monitoring has so far favoured the smaller, but more accessible Nuup Kangerlua/KNS system.

6.5. Citizen Science

INTAROS has shown that CBM data provide a valuable contribution to the knowledge on seismic shaking during e.g. earthquakes in the villages where CBM seismic sensors were installed. It is recommended to continue supporting the citizens engaging in seismic CBM.

Citizens are also involved in the collection of manual snowpack observations in the Longyeardalen valley in Svalbard. Due to the large spatial variability of snow accumulation and the paucity of automatic measurement stations, these manual observations are crucial for the Skred AS company responsible for the snow avalanche forecast in Svalbard. The manual observations, together with the automatic laser scanner data, can also be used to validate the snow maps produced with the iAOS geostatistical tool developed by ParisTech.

7. Summary

In INTAROS task 6.4 we have showcased how the iAOS can be exploited to better understand natural hazards in the Arctic by focusing on three different phenomena: snow avalanches, earthquakes, and mass loss from ice sheets and glaciers. For each hazard, we discuss the needs of various stakeholders and the work performed within the task. We illustrate how the data and methods available through the iAOS increase our understanding of the hazards, but we also identify gaps and possibilities for improvement to better fulfill stakeholder needs.

For the snow avalanche hazard in Longyearbyen the aim was to provide better forecasts of snow accumulation which in turn will help improve avalanche forecasts. We found that although surface wind can be used to predict snow erosion or accumulation, the available data is too sparse for the development of a robust statistical relationship. The geostatistical package developed in WP 5 proved to be a potentially useful tool for this purpose. However, longer time series of collocated observations are necessary for the method to be effective and realistic.

Three ocean bottom seismometer deployments have been conducted through INTAROS in seismically active areas with poor station coverage. Analysis of the collected data illustrates how even a few stations can help fill the earthquake monitoring gap in the oceans, improving both earthquake detection and source location. Long and dense timeseries of seismic events are required to assess the hazard and risk of earthquakes as needed by local authorities. Seismometers can register not only earthquakes but also landslides, snow avalanches and to some extent tsunamis. Studies focused on landslides in West Greenland show how combining seismological data with satellite observations improves the detection and understanding of such events.

The mass loss from glaciers and ice caps constitutes both global and local hazards in form of irregular sea level rise, changes in freshwater input to fjords potentially altering sea ice variability, marine ecosystems and ocean currents. Several products relating to both the total ice mass loss as well as its components have been developed using data available through the iAOS. This has resulted in new (operational) products with increased temporal and/or spatial resolution compared with previous products. To further develop models that can predict future sea level rise, our understanding of the processes involved must advance. Within task 6.4, models aimed at separating mass loss at the front of marine terminating glaciers into solid (iceberg calving) and liquid (submarine melting) parts have been developed. However, as for the snow avalanche work the lack of in-situ observations co-located in time and space, make this type of study difficult to carry out.

On the basis of the work carried out in task 6.4 we make a number of recommendations to future observing systems to the INTAROS roadmap:

- **Long timeseries (and high temporal/spatial resolution)** of observations are the backbone for quantifying the hazard and risk of natural hazards and for increased process understanding.
- Having **data freely available** through various platforms makes it easier to use, as well as visible to users from different fields.
- Creating **super sites** where multi-disciplinary data is acquired will help to overcome the problem of the lack of observations co-located in time and space and will enable the reduction of the cost/benefit ratio.

- **Providing data in real time** is important for operational services to allow authorities respond timely e.g. in the event of an earthquake or an increase in the risk of an avalanche.

8. Literature

AMAP, 2017. Snow, Water, Ice and Permafrost in the Arctic (SWIPA) 2017. Arctic Monitoring and Assessment Programme (AMAP), Oslo, Norway. xiv + 269 pp

Bengtsson, L., Andrae, U., Aspelien, T., Batrak, Y., Calvo, J., de Rooy, W., Gleeson, E., Hansen-Sass, B., Homleid, M., Hortal, M., Ivarsson, K., Lenderink, G., Niemelä, S., Nielsen, K. P., Onvlee, J., Rontu, L., Samuelsson, P., Muñoz, D. S., Subias, A., Tijm, S., Toll, V., Yang, X., & Køltzow, M. Ø. (2017). The HARMONIE–AROME Model Configuration in the ALADIN–HIRLAM NWP System, *Monthly Weather Review*, 145(5), 1919–1935. <https://doi.org/10.1175/MWR-D-16-0417.1>

Bellaire, S., Jamieson, J. B., and Fierz, C. (2011): Forcing the snow-cover model SNOWPACK with forecasted weather data, *The Cryosphere*, 5, 1115–1125, <https://doi.org/10.5194/tc-5-1115-2011>.

Bellaire, S., Jamieson, J. B., and Fierz, C. (2013): Corrigendum to "Forcing the snow-cover model SNOWPACK with forecasted weather data" published in *The Cryosphere*, 5, 1115–1125, 2011, *The Cryosphere*, 7, 511–513, <https://doi.org/10.5194/tc-7-511-2013>, 2013.

Bøssing Christensen, Ole, Drews, Martin, Hesselbjerg Christensen, Jens, Dethloff, Klaus, Ketelsen, Klaus, Hebestadt, Ines, Rinke, Anette: The HIRHAM Regional Climate Model. Version 5 (beta) , Danish Climate Centre, Danish Meteorological Institute, 2007

CARRA <https://climate.copernicus.eu/copernicus-arctic-regional-reanalysis-service>

Cornell CA (1968) Engineering seismic risk analysis. *Bull Seismol Soc Am* 58:1583–1606.

Csatho, B. M., Schenk, A. F., van der Veen, C. J., Babonis, G., Duncan, K., et al. (2014). Laser altimetry reveals complex pattern of Greenland Ice Sheet dynamics, *Proc. Natl. Acad. Sci.*, 111 (52) 18478–18483, <https://doi.org/10.1073/pnas.1411680112>

De Andrés, E., Otero, J., Navarro, F., Promińska, J., Lapazaran, J., Walczowski, W. (2018). A two-dimensional glacier–fjord coupled model applied to estimate submarine melt rates and front position changes of Hansbreen, Svalbard. *Journal of Glaciology*, 64(247), 745–758, doi: 10.1017/jog.2018.61.

De Andrés, E. , Slater, D. A., Straneo, F., Otero, J., Das, S., Navarro, F.J. (2020). Surface emergence of glacial plumes determined by fjord stratification. *The Cryosphere*, 14, 1951–1969. doi:10.5194/tc-14-1951-2020.

De Andrés, E., Otero, J., Navarro, F.J., Walczowski, W. (2021). Glacier–plume or glacier–fjord circulation models? A 2-D comparison for Hansbreen–Hansbukta system, Svalbard. *Journal of Glaciology*, First View, doi:10.1017/jog.2021.27.

Dowdeswell, J. A., Benham, T., Strozzi, T., and Hagen, J. (2008). Iceberg calving flux and mass balance of the Austfonna ice cap on Nordaustlandet, Svalbard, *Journal of Geophysical Research*, 113, F03022, doi:10.1029/2007JF000905.

Fettweis, X., Hofer, S., Krebs-Kanzow, U., Amory, C., Aoki, T., Berends, C. J., Born, A., Box, J. E., Delhasse, A., Fujita, K., Gierz, P., Goelzer, H., Hanna, E., Hashimoto, A., Huybrechts, P., Kapsch, M.-L., King, M. D., Kittel, C., Lang, C., Langen, P. L., Lenaerts, J. T. M., Liston, G. E., Lohmann, G., Mernild, S. H., Mikolajewicz, U., Modali, K., Mottram, R. H., Niwano, M., Noël, B., Ryan, J. C., Smith, A., Streffing, J., Tedesco, M., van de Berg, W. J., van den Broeke, M., van de Wal, R. S. W., van Kampenhout, L., Wilton, D., Wouters, B., Ziemen, F., Zolles, T.: GrSMBMIP: intercomparison of the modelled 1980–2012 surface mass balance over the Greenland Ice Sheet , *The Cryosphere* 14(11), 3935–3958, 2020

Gardner, A.S., G. Moholdt, J.G. Cogley, B. Wouters, A.A. Arendt, et al. (2013). A reconciled estimate of glacier contributions to sea level rise: 2003 to 2009. *Science*, 340, 852-857, <https://doi.org/10.1126/science.1234532>

Hancock, H., Prokop, A., Eckerstorfer, M., Hendrikx, J. (2018): Combining high spatial resolution snow mapping and meteorological analyses to improve forecasting of destructive avalanches in Longyearbyen, Svalbard, *Cold Regions Science and Technology*, Volume 154, Pages 120-132, <https://doi.org/10.1016/j.coldregions.2018.05.011>.

Havskov, J., Voss, P.H. and Ottemöller, L. (2020). Seismological Observatory Software: 30 Yr of SEISAN. *Seismological Research Letters*, 91 (3): 1846–1852. doi: <https://doi.org/10.1785/0220190313>

Hurkmans, R. T. W. L., Bamber, J. L., Davis, C. H., Joughin, I. R., Khvorostovsky, K. S., Smith, B. S., and Schoen, N. (2014). Time-evolving mass loss of the Greenland Ice Sheet from satellite altimetry, *The Cryosphere*, 8, 1725–1740, <https://doi.org/10.5194/tc-8-1725-2014>

Jeddi Z, Voss PH, Sørensen MB, Danielsen F, Dahl-Jensen T, Larsen TB, Nielsen G, Hansen A, Jakobsen P and Frederiksen PO (2020). Citizen Seismology in the Arctic. *Front. Earth Sci.* 8:139. doi: 10.3389/feart.2020.00139

Jeddi, Z., Ottemöller, L., Sørensen, MB., Rezaei, S., Gibbons, S.J., Strømme, M.L., Voss, P.H. and Dahl-Jensen, T. (2021). Improved Seismic Monitoring with OBS Deployment in the Arctic: A Pilot Study from Offshore Western Svalbard. *Seismological Research Letters*, accepted.

Jenkins, A. (2011) Convection-Driven melting near the grounding lines of Ice shelves and tidewater glaciers. *Journal of Physical Oceanography* 41(12), 2279–2294. doi:10.1175/JPO-D-11-03.1.

Karlsson, Nanna B, Solgaard, Anne M., Mankoff, Kenneth D., Box, Jason E, Citterio, Michele, Colgan, William T., Larsen, Signe H., Kjeldsen, Kristian K., Korsgaard, Niels J., Benn, Douglas I., Hewitt, Ian, Fausto, Robert S.: A First Constraint on Basal Melt-water Production of the Greenland Ice Sheet , *EarthArXiv Preprints* , Center for Open Science, 6 2020

Khan, S., Kjær, K., Bevis, M. *et al.* (2014). Sustained mass loss of the northeast Greenland ice sheet triggered by regional warming. *Nature Clim Change*, 4, 292–299, <https://doi.org/10.1038/nclimate2161>

Khan, S A, Jonathan L. Bamber, Eric Rignot, Veit Helm, Andy Aschwanden, David M Holland, Michiel van den Broeke, Michalea King, Brice Noël, Martin Truffer, Angelika Humbert, Saurabh Vijay, and Peter Kuipers Munneke, Greenland mass trends from airborne and satellite altimetry, *Geophysical Research Letters*, 2021, in review.

Langen, P. L., Fausto, R. S., Vandecrux, B., Mottram, R. H., and Box, J. E.: Liquid Water Flow and Retention on the Greenland Ice Sheet in the Regional Climate Model HIRHAM5: Local and Large-Scale Impacts, *Frontiers in Earth Science*, 4, <https://doi.org/10.3389/feart.2016.00110>, 2017.

Mankoff, Kenneth D., Solgaard, Anne, Colgan, William, Ahlstrøm, Andreas P., Khan, Shfaqat Abbas, Fausto, Robert S.: Greenland Ice Sheet solid ice discharge from 1986 through March 2020, *Earth System Science Data* 12(2), Copernicus GmbH, 1367–1383, 6 2020

Mankoff, Kenneth D., Noël, Brice, Fettweis, Xavier, Ahlstrøm, Andreas P., Colgan, William, Kondo, Ken, Langley, Kirsty, Sugiyama, Shin, van As, Dirk, Fausto, Robert S.: Greenland liquid water discharge from 1958 through 2019, *Earth System Science Data* 12(4), Copernicus GmbH, 2811–2841, 11 2020

Meredith, M., M. Sommerkorn, S. Cassotta, C. Derksen, A. Ekaykin, A. Hollowed, G. Kofinas, A. Mackintosh, J. Melbourne-Thomas, M.M.C. Muelbert, G. Ottersen, H. Pritchard, and E.A.G. Schuur, 2019: Polar Regions. In: IPCC Special Report on the Ocean and Cryosphere in a Changing Climate [H.-O. Pörtner, D.C. Roberts, V. Masson-Delmotte, P. Zhai, M. Tignor, E. Poloczanska, K. Mintenbeck, A. Alegría, M. Nicolai, A. Okem, J. Petzold, B. Rama, N.M. Weyer (eds.)]. In press.

Morlighem, M., Williams, C. N., Rignot, E., An, L., Arndt, J. E., Bamber, J. L., Catania, G., Chauché, N., Dowdeswell, J. A., Dorschel, B., Fenty, Ian, Hogan, K., Howat, Ian M., Hubbard, A., Jakobsson, Martin, Jordan, T. M., Kjeldsen, Kristian K., Millan, R., Mayer, L., Mouginot, J., Noël, Brice P. Y., Cofaigh, C. Ó, Palmer, S., Rysgaard, Søren, Seroussi, Héléne, Siegert, Martin J., Slabon, P., Straneo, Fiammetta, van den Broeke, Michiel R., Weinrebe, W., Wood, M., Zinglensen, K. B.: BedMachine v3: Complete bed topography and ocean bathymetry mapping of Greenland from multi-beam echo sounding combined with mass conservation, *Geophysical Research Letters* 44(21), American Geophysical Union (AGU), 11 2017

Noël, Brice, van de Berg, Willem Jan, van Wessem, J. Melchior, van Meijgaard, Erik, van As, Dirk, Lenaerts, Jan T. M., Lhermitte, Stef, Kuipers Munneke, Peter, Smeets, C. J. P. Paul, van Ulf, Lambertus H., van de Wal, Roderik S. W., van den Broeke, Michiel R.: Modelling the climate and surface mass balance of polar ice sheets using RACMO2 – Part 1: Greenland (1958–2016), *The Cryosphere* 12(3), Copernicus GmbH, 811–831, 3 2018

Otero, J., Navarro, F.J., Lapazaran, J.J., Welty, E., Puczko, D. & Finkelnburg, R. (2017). Modeling the Controls on the Front Position of a Tidewater Glacier in Svalbard. *Frontiers in Earth Science-Cryospheric Sciences*, 5, 29, doi:10.3389/feart.2017.00029.

Porter, Claire, Morin, Paul, Howat, Ian, Noh, Myoung-Jon, Bates, Brian, Peterman, Kenneth, Keeseey, Scott, Schlenk, Matthew, Gardiner, Judith, Tomko, Karen, Willis, Michael, Kelleher, Cole, Cloutier, Michael, Husby, Eric, Foga, Steven, Nakamura, Hitomi, Platson, Melisa, Wethington, Jr., Williamson, Cathleen, Bauer, Gregory, Enos, Jeremy, Arnold, Galen, Kramer, William, Becker, Peter, Doshi, Abhijit, D'Souza, Cristelle, Cummens, Pat, Laurier, Fabien, Bojesen, Mikkel: ArcticDEM , Harvard Dataverse V1, 2018, Date accessed: 2019-11-14

Prokop A., Hancock H., Praz M., Jahn E.: Slope scale avalanche forecasting in the Arctic (Svalbard), in Proceedings, International Snow Science Workshop, Innsbruck, Austria, 2018.

Rinke, A., M. Maturilli, R. M. Graham, H. Matthes, D. Handorf, L. Cohen, S. R. Hudson and J. C. Moore (2017). "Extreme cyclone events in the Arctic: Wintertime variability and trends." *Environmental Research Letters* 12(9): 094006.

Sánchez-Gómez, P., Navarro, F.J. (2018). Ice discharge error estimates using different cross-sectional area approaches: a case study for the Canadian High Arctic, 2016/17. *Journal of Glaciology*, 64(246), 595-608, doi:10.1017/jog.2018.48.

Sánchez-Gómez, P., Navarro, F., Benham, T., Glazovsky, A., Bassford, R., & Dowdeswell, J. (2019). Intra- and inter-annual variability in dynamic discharge from the Academy of Sciences Ice Cap, Severnaya Zemlya, Russian Arctic, and its role in modulating mass balance. *Journal of Glaciology*, 65(253), 780-797, doi:10.1017/jog.2019.58.

Simonsen, S. B., Barletta, V. R., Colgan, W. T., & Sørensen, L. S. (2021). Greenland Ice Sheet mass balance (1992–2020) from calibrated radar altimetry. *Geophys. Res. Lett.*, 48, e2020GL091216, <https://doi.org/10.1029/2020GL091216>

Slater, D.A., Straneo, F., Das, S.B., Richards, C.G., Wagner, T.J.W., Nienow, P.W. (2018) Localized plumes drive front-wide ocean melting of a greenlandic tidewater glacier. *Geophysical Research Letters* 45(22), 12,350–12,358. doi:10.1029/2018GL080763.

Smith, B., Fricker, H. A., Holschuh, N., Gardner, A. S., Adusumilli, S., Brunt, K. M., et al. (2019). Land ice height-retrieval algorithm for NASA's ICESat-2 photon-counting laser altimeter. *Remote Sensing of Environment*, 111352. <https://doi.org/10.1016/j.rse.2019.111352>

Svennevig, K., Munck Solgaard, A., Salehi, S., Dahl-Jensen, T., Merryman Boncori, J. P., Larsen, T. B., & Voss, P. H. (2019). A multidisciplinary approach to landslide monitoring in the Arctic: Case study of the March 2018 ML 1.9 seismic event near the Karrat 2017 landslide. *GEUS Bulletin*, 43. <https://doi.org/10.34194/GEUSB-201943-02-08>

Svennevig, K., Dahl-Jensen, T., Keiding, M., Boncori, J. P. M., Larsen, T. B., Salehi, S., Solgaard, A. M., Sørensen, M.B., Danielsen, F. and Voss, P. H. (2020). A multidisciplinary approach to landslide monitoring in the Arctic – Case study of the June 17th 2017 landslide at Karrat, West Greenland. Presented at the ESA 2020 European Polar Science Week.

Svennevig, K., Dahl-Jensen, T., Keiding, M., Merryman Boncori, J. P., Larsen, T. B., Salehi, S., Munck Solgaard, A., and Voss, P. H. (2020). Evolution of events before and after the 17 June 2017 rock avalanche at Karrat Fjord, West Greenland – a multidisciplinary approach to detecting and locating unstable rock slopes in a remote Arctic area, *Earth Surf. Dynam.*, 8, 1021–1038, <https://doi.org/10.5194/esurf-8-1021-2020>.

Sørensen, L. S., Simonsen, S. B., Nielsen, K., Lucas-Picher, P., Spada, G., Adalgeirsdottir, G., Forsberg, R., and Hvidberg, C. S. (2011). Mass balance of the Greenland ice sheet (2003–2008) from ICESat data – the impact of interpolation, sampling and firn density, *The Cryosphere*, 5, 173–186, <https://doi.org/10.5194/tc-5-173-2011>.

Sørensen, L. S., Simonsen, S. B., Forsberg, R., Khvorostovsky, K., Meister, R., and Engdahl, M. E. (2018). 25 years of elevation changes of the Greenland Ice Sheet from ERS, Envisat, and CryoSat-2 radar altimetry. *Earth and Planetary Science Letters*, 495, 234–241, <https://doi.org/10.1016/j.epsl.2018.05.015>

----- END of DOCUMENT-----



INTAROS

This report is made under the project
Integrated Arctic Observation System (INTAROS)
funded by the European Commission Horizon 2020 program
Grant Agreement no. 727890.



Project partners:



